[AMERICAN JOURNAL OF SCIENCE, SCHAIRER VOL. 267-A, 1969, P. 407-443]

HIGH-PRESSURE PHASES IN THE SYSTEM $MgO-Al_2O_3-SiO_2-H_2O$

W. SCHREYER and F. SEIFERT

Institut für Mineralogie, Ruhr-Universität Bochum, Germany

ABSTRACT. At pressures between 8 and 30 kb and temperatures of 700° to 1200°C the following compounds were synthesized within the system $MgO-Al_2O_3-SiO_2-H_2O$: Mg-staurolite, yoderite, Mg-gedrite, pyrope, and a sapphirine with the composition $Mg_2Al_4SiO_{10}$. In addition a boron-free kornerupine was synthesized for the first time. The physical constants, powder X-ray diffraction data, and the conditions for synthesis of all these phases are reported.

The tentative stability fields are as follows: Mg-staurolite is stable at fluid pressures greater than 12 kb within a temperature range that increases with pressure. At 25 kb it extends from about 750°C to 975°C. Yoderite is stable at fluid pressures between about 10 and 25 kb over a relatively narrow temperature range (about 700° to 875°C) and may become unstable at still higher pressures. Mg-gedrites as well as their Al-free equivalent anthophyllite appear to break down to other hydrous assemblages at pressures in the range 15 to 20 kb. The presumed stability field of the gedrites at lower pressures ranges from about 800° to 910°C, depending on pressure. Boron-free kornerupine appears to have a small stability field confined to the approximate range 8 to 13 kb, 850° ± 50°C. Pyrope is stable in the presence of fluid only at pressures in excess of some 15 kb and temperatures above about 750°C. The sapphirine stable at 13 kb has the composition $Mg_2Al_4SiO_{10}$, which forms cordierite and spinel at 1 atm. This sapphirine breaks down to other anhydrous phases at pressures near 24 kb and at temperatures near 950°C. At fluid pressures lower than 24 kb sapphirine breaks down to a hydrous assemblage at temperatures near 850°C. The presumably stable breakdown assemblages of all these phases are described as a function of pressure and temperature.

The possible appearance of some of these phases in addition to, or instead of, pyrope, in rocks presumed to constitute the Earth's mantle, depends largely on the compatibility relations in this system which, however, are only imperfectly known at present.

Mg-staurolite, boron-free kornerupine, and pyrope are incompatible with free quartz; yoderite, sapphirine, and Mg-gedrite may coexist with free quartz over limited pressure-temperature ranges.

INTRODUCTION

The anhydrous system $MgO-Al_2O_3-SiO_2$ was investigated at 1 atm pressure and liquidus temperatures as early as 1918 by Rankin and Merwin. Only one ternary phase, cordierite, with a composition of $2MgO \cdot 2Al_2O_3 \cdot 5SiO_2$, or close to it, was detected. Much later Foster (1950a, b) found a second ternary phase to be stable at atmospheric pressure and high temperatures: sapphirine, with a composition approximating $4MgO \cdot 5Al_2O_3 \cdot 2SiO_2$. In addition to these stable ternary phases several metastable ternary phases, forming through devitrification of glasses, were identified by Schreyer and Schairer (1961a, 1962). These metastable compounds show close structural relationships with high quartz, osumilite, and petalite.

With the addition of water to this system the number of crystalline phases is greatly increased. However, most of the newly appearing hydrous phases were found to be either Mg-silicates or Al-silicates. Thus Yoder (1952), in his study of the system $MgO-Al_2O_3-SiO_2-H_2O$ at pressures up to 2 kb, encountered only two series of quaternary phases, that is, the chlorites and talc with small Al contents later confirmed by Fawcett and Yoder (1966). In addition, Roy and Roy (1955) found that

montmorillonite may form complicated quaternary solid solutions at low temperatures.

Under high confining pressures the rarity of stable quaternary and anhydrous ternary phases is changed into an abundance. Thus a third ternary anhydrous compound, pyrope, $3MgO \cdot Al_2O_3 \cdot 3SiO_2$, becomes stable at pressures above approximately 20 kb, depending on temperature (Boyd and England, 1959), and strongly aluminous enstatites were synthesized by Boyd and England (1960a) at 18.2 kb.

More recently four new quaternary phases have been synthesized. A preliminary account of three of these syntheses has been given by Schreyer (1968) and by Schreyer and Yoder (1968). It is the purpose of the present paper to report some of the physical properties of these phases and to present the latest results bearing on their compositions and stability relations. In addition, the first synthesis of a probably hydrous, boron-free kornerupine in the system MgO–Al_2O_3–SiO_2–H_2O is described here. New data were also obtained on the anhydrous phase sapphirine.

The compound cordierite is a low-pressure phase becoming unstable at pressures near 10 kb depending on temperature It will, therefore, not be discussed in this paper, but the reader is referred to the studies by Schreyer and Yoder (1964), Schreyer (1968), and Schreyer and Seifert (1969).

The locations of crystalline phases in the system MgO–Al_2O_3–SiO_2–H_2O are shown in figure 1 in a projection from the H_2O apex of the tetrahedron onto the water-free base plane. Because of the large number of phases their compatibility relations under equilibrium conditions as a function of pressure and temperature are only partly known at present. Some compatibility triangles for probable phase relations neglecting liquids and vapors were given by Schreyer (1968); however, the kornerupine-like compound was not included. Further work in this system is still in progress.

EXPERIMENTAL PROCEDURE

The experiments were performed in two different solid-media apparatus, both of the single-stage, piston-cylinder type described by Boyd and England (1960b). Pressures were calibrated on the basis of the BiI $\rightleftharpoons$ BiII transition as shown by the same authors. Piston-out runs were made exclusively. Temperatures were measured using Pt/Pt-10 percent Rh thermocouples; however, no corrections concerning emf changes with pressure (Hannemann and Strong, 1965) were applied The furnace assemblies were slightly modified from those of Boyd and England (1961) by using crushable alumina rather than boron nitride filling rods.

Samples of 4 to 6 mg solids and 1 to 2 mg H_2O were sealed in small silver capsules with a pressed on lid. In most runs the appearance of hydrous solid phases was ample evidence that at least some water was retained in the sample; in addition, water could, in some cases, be directly observed after opening the container.

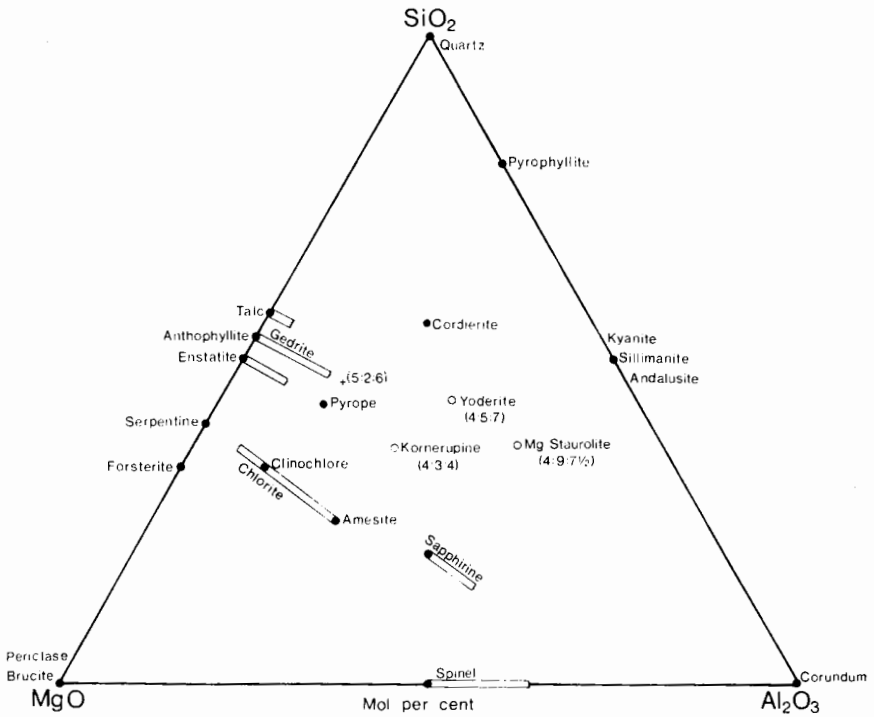

Fig. 1. Crystalline phases in the system MgO–Al_2O_3–SiO_2–H_2O projected onto the anhydrous base. Metastable phases and others stable only at low temperatures and low pressures, respectively, have been omitted. Open circles indicate phases the compositions of which are not exactly known as yet. Kornerupine stands for boron-free kornerupine.

The starting materials used for synthesis were in all but one case crystalline phases within the system studied. Previously synthesized solids made from high-purity chemicals were used where possible. In addition, carefully separated, natural Al-silicates and a chlorite were available. The following phases were mixed for the various bulk compositions studied:

Synthetic Mg-corderite crystallized from glass of the composition $2MgO \cdot 2Al_2O_3 \cdot 5SiO_2$; synthetic spinel, $MgAl_2O_4$, made and analyzed by H. R. Shell at the U. S. Bureau of Mines; pure periclase, MgO, used by Dr. J. F. Schairer at the Geophysical Laboratory; pure SiO_2 (cristobalite) also used by J F. Schairer; pure talc (U.S.P.) supplied by Mallinckrodt Chemical Works, lot No. 8476; synthetic enstatite, $MgSiO_3$, prepared from the oxides at 10 kb, 900°C; γ-Al_2O_3 prepared from Al metal; natural kyanite from Burnsville, N. C.; natural andalusite from Minas Geraes, Brazil; natural sillimanite from Benson Mines, N. Y.; natural chlorite (leuchtenbergite) from Gabbs, Nev. (Kerr and Callaghan, 1935).

In order to determine the stability limits of the new phases to be described, runs were seeded with 10 or 20 wt percent of the requisite phases that had previously been synthesized.

The run products were identified optically and by powder X-ray diffraction methods. Refractive indices were measured in Na light using immersion oils calibrated by means of an Abbé refractomer. The X-ray data were refined by the least squares method using the program for an IBM 7090 computer described by Burnham (1962). A few runs at 10 kb or below were performed in a gas-media apparatus by Dr. H. S. Yoder, Jr., using the usual sealed Pt-capsule technique.

Mg-STAUROLITE

The hitherto unknown Mg analogue of the Fe-rich staurolite series was synthesized by Schreyer (1968) at pressures between 12 and 25 kb. The success of its primary synthesis depends to a large extent on the nature of the starting materials used (table 1). Whereas mixtures of Mg-staurolite composition made up from the oxides or from MgO with mullite and aluminum silicate glass, the latter two adding up to a composition $9Al_2O_3 \cdot 8SiO_2$, failed to produce appreciable amounts of the phase, large yields were obtained from a mixture of natural kyanite + synthetic spinel + periclase at 25 kb, 850° to 900°C. Due to the similarity of the crystal structures of staurolite and kyanite, this mixture apparently provides seeds of structural units requisite for the growth of staurolite. At pressures below 15 kb, seeding with Mg-staurolite previously synthesized was necessary to achieve growth. The exact composition of staurolite is still a matter of debate. Whereas the ideal formula given by Náray-Szabó and Sasvári (1958) has an oxide ratio of $4RO \cdot 9Al_2O_3 \cdot 8SiO_2 \cdot H_2O$, Richardson (1967, 1968) in a study of pure Fe-staurolite found experimental and analytical evidence for an excess of H_2O and a deficiency of SiO_2 as compared to this ratio. His data suggest a formula of $4RO \cdot 9Al_2O_3 \cdot 7.5SiO_2 \cdot 2H_2O$. In the present study using a starting mixture of 4:9:8 ratio supporting evidence for the proposed silica-deficiency was found through the appearance of enstatite and kyanite; however, no analyses of the H_2O content of synthetic Mg-staurolite are available as yet. Despite this uncertainty, its formula was assumed, for the purpose of this paper, as $4MgO \cdot 9Al_2O_3 \cdot 7.5SiO_2 \cdot 2H_2O$.

The synthetic Mg-staurolites usually form minute, short, colorless, nearly euhedral prisms with terminal pyramid faces. They exhibit positive elongation and parallel extinction. The refractive indices are $\alpha = 1.703$ and $\gamma = 1.710$ with an error of ± 0.002. The axial angle could not be measured due to small grain size but appears to be rather large.

Powder X-ray diffraction data for synthetic Mg-staurolite are listed in table 2. Although similar to the powder pattern of Fe-rich staurolites with regard to the positions of peaks there are appreciable changes in the relative intensities. The powder pattern was indexed on the basis of an orthorhombic cell. Least squares refinement of the data led to the following cell dimensions:

$$a_o = 7.887 \pm 0.001 \text{ Å}$$
$$b_o = 16.552 \pm 0.002 \text{ Å}$$
$$c_o = 5.635 \pm 0.001 \text{ Å}$$

TABLE 1

Selected experimental results bearing on the synthesis and stability of Mg-staurolite

Fluid pressure, kb	Temp., °C	Time, hr	Condensed phases obtained
A. Starting material: Composition $4MgO \cdot 9Al_2O_3 \cdot 8SiO_2 + xH_2O$ consisting of kyanite, periclase, spinel, and 10 wt % seeds of Mg-staurolite			
12	800	20	Kyanite, talc, corundum, less staurolite
12.5	800	99	Kyanite, talc, corundum, more staurolite
13	850	26	Kyanite, corundum, gedrite, enstatite
15	700	46	Kyanite, chlorite, corundum
15	750	43	Kyanite, chlorite, corundum, same amount staurolite
15	850	5	Kyanite, talc, corundum, more staurolite, trace gedrite
15	900	2	Kyanite, enstatite, corundum
18	975	1	Corundum, enstatite, glass, trace staurolite
20	700	73	Kyanite, chlorite, corundum, less staurolite
20	975	2	Corundum, enstatite, glass
25	650	77	Kyanite, chlorite, corundum, less staurolite
25	700	23	Kyanite, chlorite, corundum, same amount staurolite
25	750	18	Kyanite, chlorite, corundum, same amount staurolite
25	900	3	Staurolite, little kyanite, enstatite, and corundum
25	975	2	Staurolite, pyrope, kyanite, corundum
25	1000	2	Pyrope, kyanite, corundum, trace staurolite, some montmorillonite (quenched fluid)
B. Starting material: Composition $3MgO \cdot 3Al_2O_3 \cdot 5SiO_2 + xH_2O$ consisting of cordierite and spinel, no seeds			
20	950	1	Staurolite, enstatite, glass
C. Starting material: Composition $4MgO \cdot 9Al_2O_3 \cdot 8SiO_2 + xH_2O$ consisting of periclase, mullite, and aluminum silicate glass, the latter two adding up to a composition $9Al_2O_3 \cdot 8SiO_2$; no seeds			
20	850	4	Yoderite, corundum
D. Starting material: Composition $4MgO \cdot 9Al_2O_3 \cdot 8SiO_2 + xH_2O$ consisting of kyanite, periclase, spinel, no seeds			
25	850	16	Staurolite, traces kyanite and enstatite
E. Starting material: Composition $4MgO \cdot 9Al_2O_3 \cdot 8SiO_2 + xH_2O$ consisting of periclase, γ-Al_2O_3, and cristobalite			
20	950	2	Enstatite, corundum, glass

TABLE 2

Powder X-ray diffraction data for synthetic Mg-staurolite prepared at 25 kb, 850°C, 22 hours, and rerun at 18 kb, 950°C, 1 hour (internal Si standard, CuKα radiation)

hkl	$2\theta_{observed}$	I/I_o	$d_{observed}$	d_{calc}	$\Delta Q \times 10^5$
1 3 0	19.64	17	4.520	4.5209	2
1 1 1	20.09	15	4.420	4.4186	-3
0 4 0	21.46	63	4.141	4.1380	-7
2 0 0	22.58	2	3.938	3.9434	19
2 2 0	25.03	25	3.558	3.5599	11
1 3 1	25.25	33	3.527	3.5263	-3
2 0 1	27.61	25	3.231	3.2309	1
1 5 0	29.24	4	3.054	3.0524	-13
2 2 1	29.68	39	3.010	3.0100	-2
2 4 0	31.32	9	2.856	2.8547	-11
0 0 2	31.75	10	2.818	2.8176	-6
0 6 0	32.43	49	2.761	2.7587	-19
1 5 1	33.37	73	2.685	2.6839	-11
1 1 2	34.21	5	2.621	2.6199	-12
3 1 0	34.54	9	2.597	2.5964	-4
2 4 1	35.23	12	2.547	2.5466	-10
1 3 2	37.62	66	2.391	2.3912	4
3 3 0	37.92	40	2.373	2.3733	9
3 1 1	38.17	34	2.358	2.3581	6
0 4 2	38.65	6	2.330	2.3289	-9
2 0 2	39.31	10	2.292	2.2925	10
2 6 0	39.88	19	2.261	2.2604	0
1 7 1	43.05	25	2.101	2.1016	10
0 8 0	43.77	4	2.068	2.0690	18
3 5 0	43.98	4	2.059	2.0587	-2
2 4 2	45.18	2	2.007	2.0053	-38
4 0 0 0 6 2	46.04	100	1.971	1.9717 1.9712	9 -5
4 0 1	48.88	3 B	1.863	1.8611	-68
4 4 0	51.33	2	1.7799	1.7800	1
2 8 1	52.52*	21	1.7409	1.7424	55
1 9 1	53.69	12	1.7071	1.7069	-9
3 5 2 2 2 3	55.29	5	1.6615	1.6623 1.6613	36 -6
0 10 0	55.45*	5	1.6557	1.6552	-20
1 5 3	57.58*	10 B	1.5994	1.5997	19
2 4 3	58.83	1	1.5696	1.5692	-25
4 6 1	59.95	5	1.5430	1.5428	-9
2 8 2	60.24	8	1.5362	1.5360	-15
1 9 2	61.27*	23	1.5116	1.5115	-4
2 10 1 3 3 3	63.04*	4	1.4733	1.4731 1.4729	-13 -29
2 6 3	64.44*	6	1.4447	1.4447	1
5 5 0	65.50*	1	1.4238	1.4240	10
0 0 4	66.32*	14	1.4082	1.4088	42
4 6 2	67.12*	55	1.3934	1.3940	49
0 12 0	67.91*	29	1.3791	1.3793	21

*For these peaks the $CuK\alpha_1$ reflections were measured and used in the calculations.

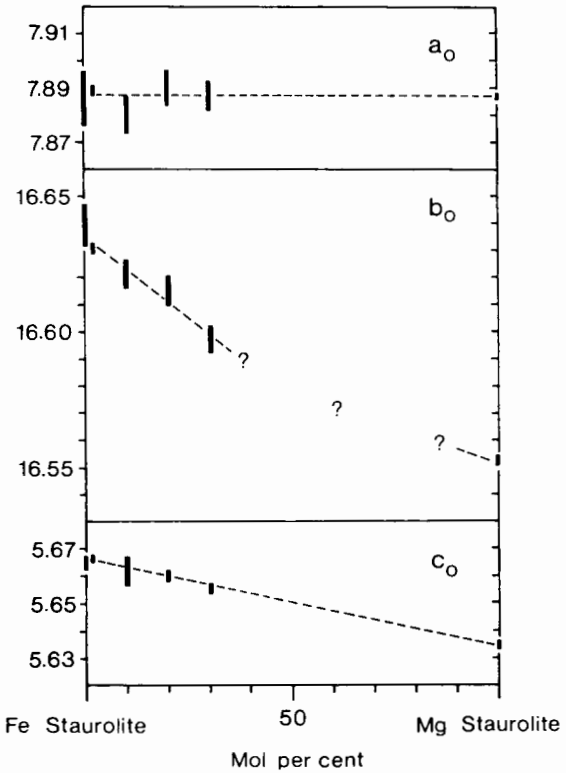

Fig. 2. Unit cell parameters of staurolites in the system Fe staurolite-Mg staurolite. The data for the Fe-rich members were taken from Richardson (1967).

These values are plotted in figure 2 together with those obtained by Richardson (1967) on Fe-rich members within the system Fe-staurolite–Mg-staurolite. Whereas substitution of Mg for Fe^{+2} causes virtually no change in the a_o dimension, there is, in agreement with Richardson (1967), an obvious contraction of the structure in both the b and c directions. For b_o the relationship cannot be linear over the entire compositional range. The density calculated from X-ray data was found to be 3.54.

The tentative stability field of Mg-staurolite based on the data compiled in table 1 is wedge shaped (fig. 3), increasing in width with pressure. It is probable that the directly adjoining, low-temperature breakdown assemblage, over the entire pressure range investigated, is kyanite + chlorite + corundum. Because the join chlorite–kyanite appears to be stable under these conditions, the phases yoderite and pyrope, even if stable on their own compositions, are unlikely to appear as low-temperature breakdown products of Mg-staurolite in the presence of excess H_2O.

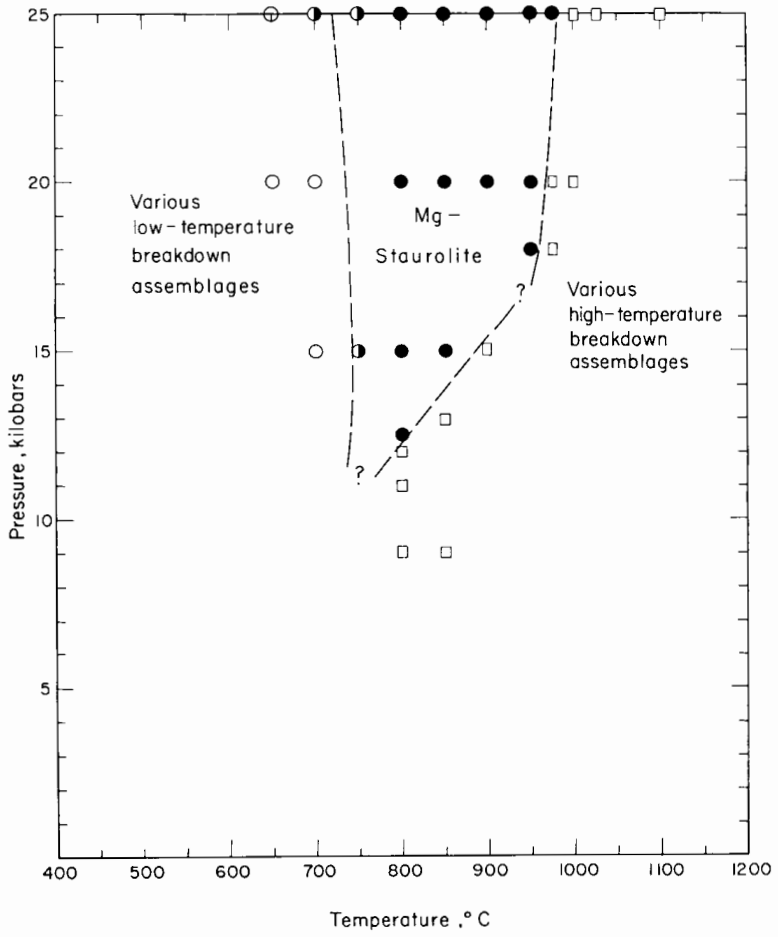

Fig. 3. Preliminary pressure-temperature diagram for the stability field of Mg-staurolite in the presence of excess fluid based on runs seeded with synthetic Mg-staurolite. Solid dots indicate growth of Mg-staurolite; open circles, breakdown to the low-temperature assemblage chlorite + kyanite + corundum; open boxes, breakdown to high-temperature assemblages as discussed in the text. Composite symbols indicate negligible reaction of the Mg-staurolite seeds.

The upper temperature stability limit of Mg-staurolite shows at least one obvious change in slope, which is probably due to the appearance of pyrope in addition to kyanite + corundum as breakdown products at pressures above approximately 16 kb. Below this pressure the stable breakdown reactions are not as yet fully understood, because some of the assemblages obtained consisted of too many phases and were, therefore, metastable. It will be necessary to seed the runs with all the possible breakdown assemblages. Thus far, with decreasing pressures and temperatures the breakdown assemblages enstatite + corundum +

liquid, enstatite + corundum + kyanite, and yoderite + corundum + kyanite are envisaged.

The inferred assemblage yoderite + corundum + kyanite is particularly interesting inasmuch as it is related to the low-temperature breakdown assemblage chlorite + corundum + kyanite by the reaction chlorite + kyanite $\rightleftharpoons$ yoderite + corundum + H_2O. The univariant curve for this reaction is one of the five curves originating from an invariant point which may well designate the low-pressure end of the wedge-shaped Mg-staurolite stability range in the presence of excess fluid. The theoretical relations in the vicinity of this invariant point are shown in figure 4. From the two reactions producing Mg-staurolite near this invariant point only one, that is, chlorite + kyanite + corundum $\rightleftharpoons$ staurolite + H_2O, releases water and must, therefore, proceed to the right with increasing temperature. On the other hand, the reaction yoderite + kyanite + corundum $\rightleftharpoons$ staurolite probably does not involve a change in H_2O content of the solid assemblages, or only a very slight change depending on the precise composition of the yoderite and Mg-staurolite. For this reason, the requisite univariant curve in figure 4 may have a very flat slope which is largely governed by the entropy and volume changes of the solid phases alone. Whereas the influence of entropy cannot be evaluated at present, it was found by calculation that the assemblage yoderite + kyanite + corundum is slightly less dense than Mg-staurolite itself and may, therefore, represent the low-pressure breakdown assemblage of Mg-staurolite. The dot-dashed portion of the univariant curve (Chl, V) as shown on the left side of figure 4 represents a metastable extension for the conditions of excess fluid. However, under conditions of water-deficiency, this portion of the curve becomes stable thus indicating that, in the water-deficient region (Yoder, 1952), Mg-staurolite will be stable to lower temperatures and, possibly, pressures than shown in figure 3.

Concerning the compatibility of Mg-staurolite with other phases in the system MgO–Al_2O_3–SiO_2–H_2O, the most important observation is that, unlike the Fe-rich staurolites, it cannot coexist with free quartz in any portion of the pressure temperature-range investigated. For this reason the appearance of Mg-staurolite with or without other crystalline phases is confined to highly aluminous bulk compositions.

YODERITE

A pure Mg end member of the natural mineral yoderite, discovered by McKie (1959), was synthesized by Schreyer and Yoder (1968). It grows readily at pressures between 11 and 25 kb over a wide temperature range, provided mixtures of corderite and spinel with or without andalusite are used as a starting material (table 3). However, over at least half of this growth field yoderite is a metastable substitute for the structurally related kyanite. Starting materials containing kyanite yield yoderite only when seeded with the latter phase and then exclusively within the supposed stability field for yoderite (Schreyer and Yoder, 1968).

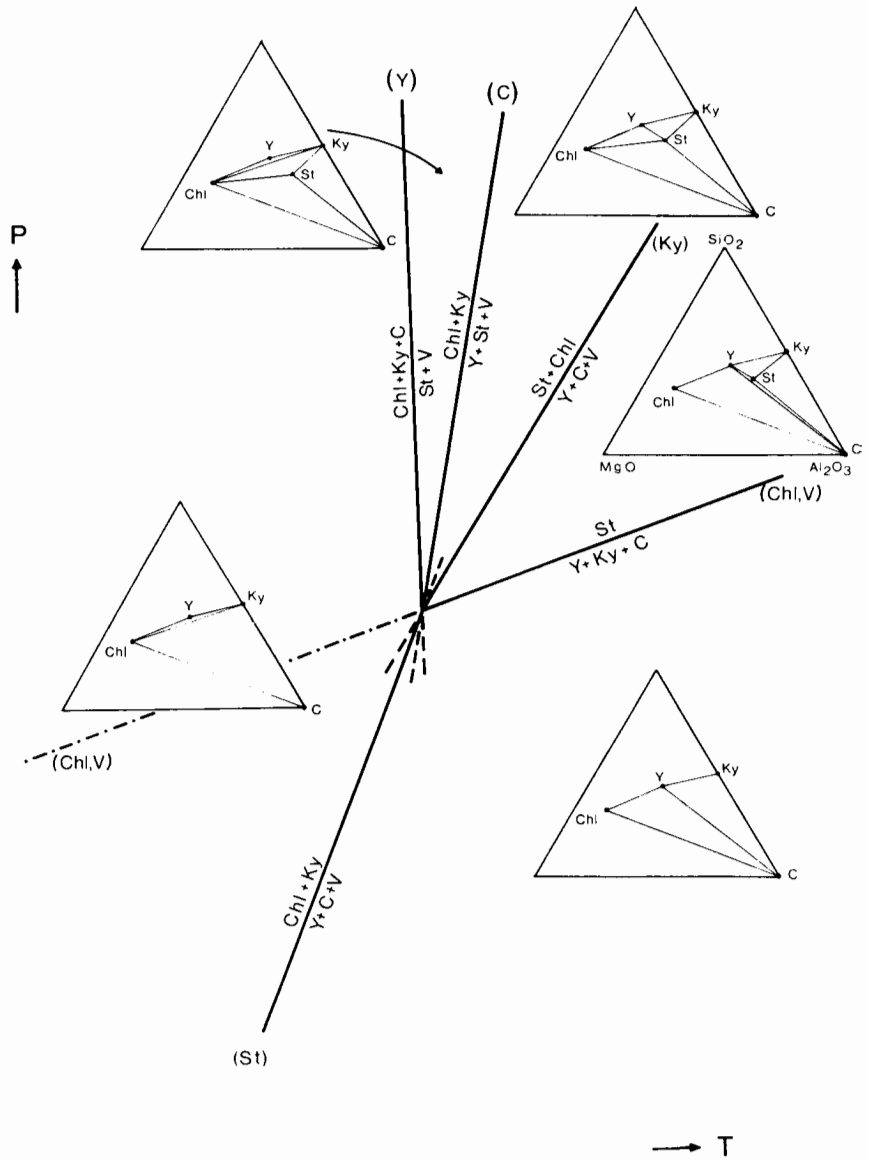

Fig. 4. Distribution of univariant curves around the invariant point involving the phases Mg-staurolite (St), kyanite (Ky), chlorite (Chl), corundum (C), yoderite (Y), and vapor (V). The abbreviations given in the diagram in parentheses indicate the absent phase for the particular reaction. Slopes are tentative.

TABLE 3

Selected experimental results bearing on the synthesis and stability of yoderite

Fluid pressure, kb	Temp., °C	Time, hr	Condensed phases obtained
A. Starting material: Composition $4MgO{\cdot}5Al_2O_3{\cdot}7SiO_2 + xH_2O$ consisting of kyanite, talc, chlorite, and 10 wt % yoderite seeds			
10*	600	168	Kyanite, chlorite, trace quartz
10*	800	72	Yoderite, talc, corundum, kyanite
11	700	48	Kyanite, chlorite, talc, same amount yoderite
11	800	69	Talc, corundum, kyanite, more yoderite
15	700	29	Kyanite, chlorite, talc, small trace yoderite
15	750	24	Kyanite, chlorite, talc, same amount yoderite
15	800	21	Kyanite, chlorite, talc, more yoderite
20	700	24	Kyanite, chlorite, talc
20	800	19	Kyanite, chlorite, talc, same amount yoderite
20	850	19	Yoderite, staurolite, kyanite, little gedrite, and enstatite
20	900	2	Staurolite, enstatite, kyanite, same amount yoderite
20	950	1	Enstatite, corundum, kyanite, staurolite
25	700	21	Kyanite, chlorite, talc
25	800	19	Kyanite, chlorite, talc, staurolite, more yoderite
25	900	1	Staurolite, kyanite, enstatite
B. Starting material: Composition $4MgO{\cdot}5Al_2O_3{\cdot}7SiO_2 + xH_2O$ consisting of talc, corundum, yoderite, trace sillimanite			
11	850	21	Yoderite, corundum, gedrite, trace enstatite
11	900	2	Enstatite, corundum, little montmorillonite (quenched fluid)
15	900	3	Enstatite, corundum, little montmorillonite (quenched fluid)
C. Starting material: Composition $4MgO{\cdot}5Al_2O_3{\cdot}7SiO_2 + xH_2O$ consisting of cordierite, spinel, and andalusite; no yoderite seeds			
15	800	3	Yoderite, trace talc
18	800	16	Yoderite, staurolite, talc, little corundum
D. Starting material: Composition $2MgO{\cdot}2Al_2O_3{\cdot}3SiO_2 + xH_2O$ consisting of cordierite and spinel; no yoderite seeds			
20	800	5	Yoderite, little talc and chlorite
25	700	3	Yoderite, staurolite, talc, trace chlorite
E. Starting material: Composition $3MgO{\cdot}3Al_2O_3{\cdot}5SiO_2 + xH_2O$ consisting of cordierite and spinel; no yoderite seeds			
11	800	65	Cordierite, spinel, corundum, talc, quartz, little yoderite
15	600	17	Yoderite, chlorite, quartz, corundum
15	800	19	Yoderite, traces talc and montmorillonite
15	900	1	Yoderite, little enstatite, glass
20	850	1	Yoderite, traces talc and enstatite
F. Starting material: Composition $2MgO{\cdot}3Al_2O_3{\cdot}4SiO_2 + xH_2O$ consisting of cordierite, spinel, andalusite; no yoderite seeds			
15	800	3	Yoderite, little talc, trace corundum
20	800	17	Yoderite, staurolite, talc
G. Starting material: Composition $5MgO{\cdot}5Al_2O_3{\cdot}7SiO_2 + xH_2O$ consisting of kyanite and chlorite, no yoderite seeds			
15	800	19	Kyanite, chlorite, talc, staurolite

*Runs performed in gas apparatus.

TABLE 4

Powder X-ray diffraction data for two yoderites: (1) synthetic, prepared at 16 kb, 800°C, 17 hours; (2) natural, purple variety, from Mautia Hill, Tanzania (internal Si standard, $CuK\alpha_1$ radiation*)

hkl	Synthetic					Natural				
	$2\theta_{observed}$	I/I_o	$d_{observed}$	d_{calc}	$\Delta Q \times 10^5$	$2\theta_{observed}$	I/I_o	$d_{observed}$	d_{calc}	$\Delta Q \times 10^5$
001	12.67	10	6.981	6.972	-5					
110	19.07	13	4.650	4.636	-28	19.12	9	4.639	4.643	+7
$11\bar{1}$						21.26	2	4.177	4.174	-7
200	23.03	5	3.859	3.859	+2	22.99	6	3.865	3.869	+14
$20\bar{1}$	23.26	5	3.821	3.818	-11	23.24	8	3.824	3.824	0
111	24.65	15	3.608	3.612	+13	24.56	10	3.622	3.622	+2
002	25.53	100	3.486	3.486	-1	25.44	100	3.498	3.499	+5
210	27.76	16	3.211	3.213	+10	27.72	31	3.216	3.219	+21
$21\bar{1}$	27.96	13	3.188	3.189	+2	27.92	24	3.193	3.193	-1
201	29.16	9	3.060	3.059	-3	29.06	10	3.071	3.071	+1
$11\bar{2}$	29.58	69	3.017	3.019	+13	29.49	55	3.026	3.026	0
$20\bar{2}$						29.72	19	3.003	3.005	+12
102	30.70	15	2.910	2.909	-9	30.58	6	2.921	2.921	+6
020	30.81	11	2.900	2.899	-4	30.76	22	2.904	2.902	-17
120	32.95	1	2.716	2.714	+22	32.93	6	2.717	2.717	-5
211	33.06	2	2.707	2.706	-14					
021	33.49	10	2.673	2.677	+36	33.39	17	2.681	2.681	-6
$30\bar{1}$	33.89	3	2.643	2.645	+19	33.80	7	2.650	2.649	-3
112	34.46	39	2.600	2.600	-6	34.30	46	2.612	2.609	-31
300	34.84	17	2.573	2.573	-2	34.75	42	2.579	2.579	+1
121	36.59	1	2.454	2.455	+19	36.48	23	2.461	2.460	-18

TABLE 4 (continued)

hkl	Synthetic					Natural				
	$2\theta_{observed}$	I/I_o	$d_{observed}$	d_{calc}	$\Delta Q \times 10^5$	$2\theta_{observed}$	I/I_o	$d_{observed}$	d_{calc}	$\Delta Q \times 10^5$
$31\bar{1}$	37.34	2	2.406	2.406	-1	37.27	4	2.411	2.410	-9
$30\bar{2}$						37.64	22	2.388	2.388	-3
310	38.23	5	2.352	2.352	-9	38.12	9	2.359	2.357	-26
$20\bar{2}$	38.99	20	2.308	2.308	+4	38.82	9	2.318	2.318	0
$20\bar{3}$	39.78	11	2.264	2.265	+13	39.65	7	2.271	2.270	-12
301	40.30	14	2.236	2.234	-32	40.17	27	2.243	2.242	-14
022	40.46	12	2.228	2.229	+27	40.40	4	2.230	2.234	+59
$11\bar{3}$	40.59	6	2.221	2.219	-24					
$31\bar{2}$	40.96	2	2.201	2.204	+56	40.79	1	2.211	2.208	-44
013	41.86	1	2.156	2.157	+18					
$21\bar{2}$	42.11	6	2.144	2.145	+13	41.90	4	2.154	2.152	-29
$21\bar{3}$	42.82	7	2.110	2.110	-11	42.73	5	2.114	2.114	-6
122	44.09	1	2.052	2.053	+27	43.91	2	2.060	2.059	-30
$30\bar{3}$						45.28	5	2.001	2.003	+51
$31\bar{3}$	48.14	4	1.889	1.890	+40	48.04	8	1.892	1.893	+43
410	49.73	1	1.832	1.831	-34					
023	50.29	34	1.813	1.813	+18	50.11	33	1.819	1.818	-26
$22\bar{3}$						51.01	1	1.789	1.788	-31
401	52.29	1	1.748	1.748	-14	52.05	2	1.755	1.753	-60
004	52.44	2	1.743	1.743	-13	52.19	2	1.751	1.750	-59

*Possible errors in the d values caused by the failure to recognize $K\alpha_1$ reflections at low angles 2θ are eliminated by the Si standard also defined on the basis of $K\alpha_1$ throughout the pattern.

Because complete reaction was never observed, and no analytical data are available, the exact composition of the yoderite synthesized is not known. However, from the phase assemblages obtained, it is likely, that it lies within the range given by the anhydrous compositions $2MgO \cdot 2Al_2O_3 \cdot 3SiO_2$, $4MgO \cdot 5Al_2O_3 \cdot 7SiO_2$, and $3MgO \cdot 3Al_2O_3 \cdot 5SiO_2$. For the purpose of this paper the formula $Mg_4Al_{10}Si_7O_{31}(OH)_4$ was assumed; this formula has a relative water content very close to that determined by McKie (1959) for natural purple yoderite and identical to that of the more recently discovered green yoderite variety (McKie and Bradshaw, 1966). It is possible that the synthetic yoderites exhibit binary or even ternary solid solution.

The synthetic yoderites, if well developed, form colorless monoclinic blades. Because of the small size no single crystal studies have been made on the synthetic material; the observable crystal faces could, therefore, not be indexed on the basis of the unit cell proposed by McKie (1959). However, U-stage measurements indicate that the blades are elongated along the b-direction of that cell with length slow when lying on the prominent pinacoid face of the zone [010]. The optic axial plane is (010), and $2V_z = 60° \pm 5°$ is surprisingly high compared with McKie's (1959) value for natural yoderite of 25°. Because of the morphology of the yoderite crystals only one index of refraction could be measured: $\beta = 1.678 \pm 0.003$. The birefringence is estimated to be 0.020.

Powder X-ray diffraction data for a synthetic yoderite prepared from a starting composition of $4MgO \cdot 5Al_2O_3 \cdot 7SiO_2$ plus water are given in table 4 together with new data on a natural purple yoderite from Mautia Hill, Tanzania, separated by Dr. H. S. Yoder, Jr., at the Geophysical Laboratory, Washington, D. C. The powder pattern of yoderite given by McKie (1959) was not indexed. These reflections were indexed, however, in the ASTM catalogue, card no. 12-625, assuming superstructure reflections of appreciable intensity. Accepting this indexing Schreyer and Yoder (1968) had compared these superstructure reflections with the non-Bragg reflections originally described by McKie (1959) on the basis of single crystal work. Therefore, they had concluded that the powder X-ray diffraction pattern of synthetic yoderite exhibited the same non-Bragg reflections as the natural mineral. In the present study, however, the ASTM indexing was found to be largely erroneous: Using these indices no refinement of the lattice constants was possible for the synthetic yoderite. On the other hand, all observed reflections of both the synthetic and the natural yoderites could be used for refinement when different indices based entirely upon the small monoclinic cell proposed by McKie (1959) were applied. Therefore, in contrast to the statement made by Schreyer and Yoder (1968) the powder X-ray diffraction patterns of synthetic as well as natural yoderites do not support conclusions concerning supercells. The question as to whether or not synthetic yoderite exhibits a supercell similar to that found for the natural material can only be resolved by single crystal methods.

The cell dimensions of the two yoderites studied, refined by the least-squares method, are given in table 5 and compared with other data on natural purple yoderite. It is apparent that the synthetic and natural yoderites studied here have very similar cell dimensions. However, the cell dimensions for the natural yoderite obtained in the present study differ considerably from those determined by McKie (1959) as well as by Fleet and Megaw (1962) from single crystal work. This is especially surprising inasmuch as the powder data compiled in table 4 are very close to those measured by McKie (1959). Yet, differences in the bulk compositions of the various samples of natural yoderites studied, and small systematic errors not included in the limits of error given by the various authors may, of course, be the reason for these discrepancies. The density of the synthetic yoderite was calculated from the X-ray data on the basis of the assumed formula $Mg_4Al_{10}Si_7O_{31}(OH)_4$, transformed for the proper oxygen content per unit cell (20 after McKie, 1959; Fleet and Megaw, 1962) into $Mg_{2.28}Al_{5.72}Si_{4.00}O_{17.72}(OH)_{2.28}$, and found to be 3.31.

TABLE 5

Comparison of lattice constants of synthetic and natural yoderites

Sample	a_o, Å	b_o, Å	c_o, Å	β
Synthetic (this study; see table 4)	7.987 ± 0.002	5.798 ± 0.002	7.214 ± 0.002	104.90 ± 0.02
Natural purple (this study; see table 4)	8.003 ± 0.003	5.804 ± 0.002	7.238 ± 0.003	104.77 ± 0.03'
Natural purple (McKie, 1959)	8.10 ± 0.05	5.78 ± 0.05	7.28 ± 0.05	106 ± 1°
Natural purple (Fleet and Megaw, 1962)	8.035 ± 0.003	5.805 ± 0.001	7.346 ± 0.002	105°38' ± 4'

On the basis of the experimental results compiled in table 3 synthetic Mg-yoderite seems to exhibit a narrow thermal stability range between approximately 700° and 875°C. The pressure stability is rather extensive ranging from some 9 kb to at least 25 kb (Schreyer and Yoder, 1968). The low-temperature breakdown products over a large pressure range above 10 kb are chlorite + talc + kyanite. However, there are indications that at pressures between 20 and 25 kb the lower temperature stability limits of yoderite and pyrope intersect thus generating an invariant point involving the phases yoderite, pyrope, chlorite, kyanite, talc, and vapor. The theoretical phase relations in the vicinity of this invariant point are depicted in figure 5. They imply a breakdown reaction of yoderite

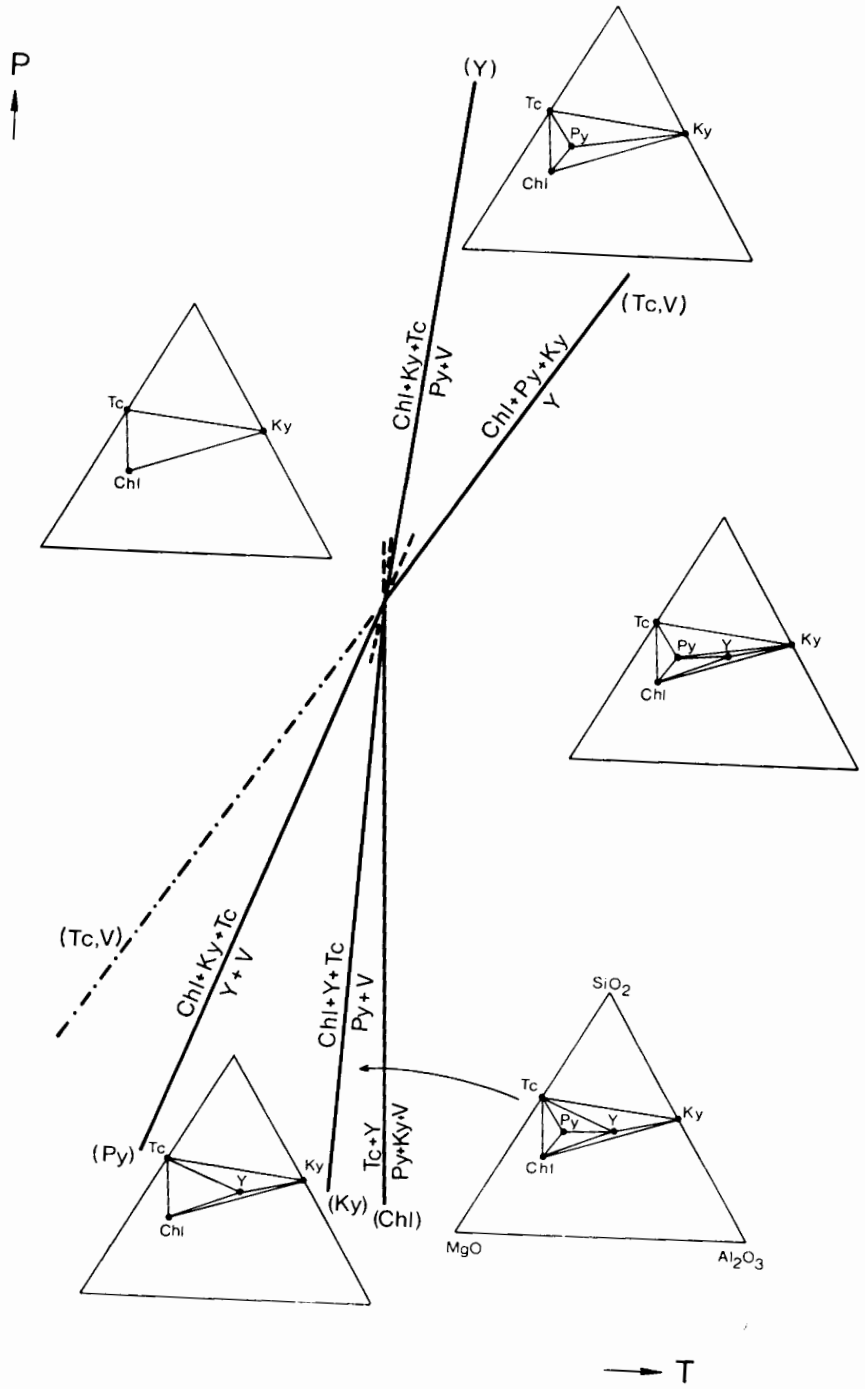
P
T
(Y)
(Tc,V)
(Tc,V)
(Py)
(Ky)
(Chl)
Chl+Ky+Tc
Py+V
Chl+Py+Ky
Y
Chl+Ky+Tc
Y+V
Chl+Y+Tc
Py+V
Tc+Y
Py+Ky+V
Tc
Py
Ky
Chl
Y
SiO2
MgO
Al2O3

into chlorite + kyanite + pyrope at pressure-temperature conditions to the left of the univariant curve marked (Tc, V). In this reaction the water content of the solid assemblages remains unchanged, but there is a small increase in density toward the pyrope-bearing assemblage. Under these circumstances, the reaction curve, by virtue of a relatively flat slope, as shown in figure 5, might effectively be an upper pressure limit of yoderite. Such behavior would explain the experimental observation that yoderite formation is more sluggish at 25 kb than at 15 kb. Experiments using seeded starting materials may resolve this point. Similarly as in figure 4 the solid curves apply exclusively to conditions with excess water vapor (fluid), whereas the dot-dashed curve is only stable in the water deficient-region. In the latter case, therefore, yoderite may be stable to lower temperatures than with excess water present.

A high-temperature breakdown of yoderite into kyanite + enstatite + Mg-staurolite was observed at pressures in excess of 15 kb. Toward lower pressures the stable breakdown assemblage appears to be kyanite + enstatite + corundum. This change is probably due to the intersection of the upper stability limits of yoderite and Mg-staurolite thereby producing an invariant point involving the phases yoderite, Mg-staurolite, kyanite, enstatite, corundum, and vapor.

The stability field of yoderite is terminated toward lower pressures by breakdown reactions producing higher volume assemblages, which contain, in most cases, the low-pressure phase cordierite. Phase relations are complicated because of the large number of reactions taking place: There are probably at least five stable invariant points in the pressure range 8 to 11 kb. The final closure of the yoderite field may result from the intersection of the univariant curves of the two reactions:

(1) 33 kyanite + 6 chlorite + 1 cordierite = 8 yoderite + 8.5 H_2O

(2) 23 cordierite + 43 corundum + 6 chlorite + 2.5 H_2O = 19 yoderite

Because water release accompanies the formation of yoderite in equation (1), yoderite is stable on the high-temperature side of the requisite univariant curve. Conversely, yoderite is likely to be the low-temperature phase in equation (2), in which water is being consumed with the formation of yoderite assuming a water content of the cordierite of 0.5 H_2O per formula unit. The intersection of the two curves is marked by an invariant point involving the phases cordierite, kyanite, chlorite, corundum, yoderite, and vapor. The breakdown reactions of yoderite at pressures below 10 kb are presently being studied experimentally in cooperation with Dr. H. S. Yoder, Jr.

Over the largest part of its stability field, the compatibility relations of yoderite with other crystalline phases in the system MgO–Al_2O_3–SiO_2–H_2O are comparable with those found for Mg-staurolite However, whereas Mg-staurolite cannot coexist with free quartz under any of the condi-

---

Fig. 5. Distribution of univariant curves around the invariant point involving the phases chlorite (Chl), talc (Tc), kyanite (Ky), yoderite (Y), pyrope (Py), and vapor (V). The abbreviations given in the diagram in parentheses indicate the absent phase for the particular reaction. Slopes are tentative.

tions studied, a very small field for yoderite + quartz was found by Schreyer and Yoder (1968) near 10 kb, 700°C. The assemblage yoderite + quartz is also encountered in the only known natural occurrence of yoderite at Mautia Hill, Tanzania (McKie, 1959).

SAPPHIRINE

The synthesis of sapphirine at elevated pressures has been reported in recent years by a number of authors (for example, Boyd and England, 1959 and 1963; Schreyer and Yoder, 1960 and 1964; Schreyer, 1968); little is known, however, about its composition and stability.

In the present study (see table 6) a sapphirine was synthesized in the presence of water from a composition $2MgO \cdot 2Al_2O_3 \cdot SiO_2$ at 13 kb and 900°C using a starting mixture of synthetic cordierite plus synthetic $MgAl_2O_4$ spinel. Traces of corundum and spinel were detected in addition to sapphirine; these can be explained as products of preferred leaching of silica and Mg by the vapor phase. It is thus believed that the sapphirine synthesized has indeed the composition of the solid starting material, that is, $Mg_2Al_4SiO_{10}$. This composition is also closely approached in some natural sapphirines (Vogt, 1947; Segnit, 1957). On the other hand sapphirines synthesized at atmospheric pressure and higher temperatures in the dry system MgO–Al_2O_3–SiO_2 by Foster (1950a, b) and by Keith and Schairer (1952) were invariably more aluminous, probably due to a partial substitution of $AlAl \rightleftharpoons MgSi$ (Kuzel, 1961). Such more aluminous sapphirines are also found in nature (see Vogt, 1947). These experimental observations suggest that the extent of solid solution in sapphirine is pressure sensitive with increasing pressures stabilizing less aluminous compositions. This behavior is the opposite to that observed for aluminous enstatite (Boyd and England, 1960a) in the same pressure range.

The sapphirine, $Mg_2Al_4SiO_{10}$, could also be synthesized at 10 kb, 900°C, that is under conditions within the stability field of cordierite. This sapphirine lies on the join cordierite–spinel, which is stable at 1 atm (Schreyer and Schairer, 1961b); thus, with increasing MgSi solid solution in sapphirine, this join is broken at some pressure between 1 bar and 10 kb by the reaction already outlined by Vogt (1947):

$$\underset{\text{cordierite}}{Mg_2Al_4Si_5O_{18}} + 8\underset{\text{spinel}}{MgAl_2O_4} = 5\underset{\text{sapphirine}}{Mg_2Al_4SiO_{10}}$$

These results are in agreement with the earlier observation made by Schreyer and Yoder (1960) that cordierite itself breaks down in the absence of water at 10 kb and temperatures of 1200°C or higher to only sapphirine + quartz.

Optically the 2:2:1 sapphirine forms a dense aggregate of extremely fine-grained, anhedral crystals too small for optical measurements. Only the mean index of refraction could be determined: 1.699 ± 0.003.

Powder X-ray diffraction data for the synthetic sapphirine $Mg_2Al_4SiO_{10}$ are presented in table 7 together with data on an aluminous

sapphirine close to the composition $4MgO \cdot 5Al_2O_3 \cdot 2SiO_2$ made at atmospheric pressure by W. R. Foster. There are measurable differences in the peak locations of the two specimens. All reflections could be indexed on the basis of monoclinic cells with the orientation originally given by Gossner and Mussgnug (1928) and also chosen by McKie (1963) and Fleet (1967). One of the salient features of carefully measured sapphirine powder patterns is the close proximity or coincidence of many observed and possible reflections, which might indicate a pseudosymmetry in this mineral. Due to the multitude of peaks the powder pattern was indexed to d-values only as low as 2.30. In table 8 the lattice constants of the two sapphirines studied are compared. For the new $Mg_2Al_4SiO_{10}$ sapphirine c_o has decreased, whereas b_o has markedly increased in comparison to the sapphirine synthesized at 1 atm.

TABLE 6

Selected experimental results bearing on the synthesis and stability of sapphirine

Fluid pressure, kb	Temp., °C	Time, hr	Condensed phases obtained
A. Starting material: Composition $2MgO \cdot 2Al_2O_3 \cdot SiO_2 + xH_2O$ consisting of cordierite and spinel			
13	800	43	Chlorite, corundum, traces of spinel and cordierite
13	900	18	Sapphirine, traces spinel and corundum
19.5	900	5	Spinel, enstatite, corundum, trace sapphirine
19.5	900	22	Sapphirine, spinel, enstatite, corundum
B. Starting material: Composition $2MgO \cdot 2Al_2O_3 \cdot SiO_2 + xH_2O$ consisting of enstatite, corundum, spinel, and 20 wt % sapphirine			
22	950	10	More sapphirine, spinel, corundum, little enstatite
26	900	21	Enstatite, spinel, corundum
30	950	17	Pyrope, spinel, corundum
C. Starting material: Synthetic sapphirine (Foster) with a composition close to $4MgO \cdot 5Al_2O_3 \cdot 2SiO_2$			
15	800	46	Chlorite, corundum, little sapphirine
20	800	22	Chlorite, corundum, sapphirine
D. Starting material: Composition $4MgO \cdot 5Al_2O_3 \cdot 7SiO_2 + xH_2O$ consisting of chlorite, sillimanite, cordierite, and 10 wt % yoderite			
8*	800	168	Sapphirine, cordierite, corundum

*Run performed in gas apparatus.

It is interesting to note that the phase sapphirine is not stable at very high confining pressures. Preliminary runs seeded with synthetic sapphirine (see table 6) indicate that it breaks down to the assemblage pyrope + corundum + spinel at pressures near 24 kb and temperatures of about 950°C.

TABLE 7

Powder X-ray diffraction data for two synthetic sapphirines: (1) $Mg_2Al_4SiO_{10}$ prepared at 900°C, 13 kb (this study); (2) aluminous sapphirine prepared by Foster (no. 8119) at 1 atm (internal Si standard, $CuK\alpha_1$ radiation, see table 2)

hkl	$Mg_2Al_4SiO_{10}$ (this study)					Aluminous sapphirine (Foster)				
	$2\theta_{observed}$	I/I_o	$d_{observed}$	d_{calc}	$\Delta Q \times 10^5$	$2\theta_{observed}$	I/I_o	$d_{observed}$	d_{calc}	$\Delta Q \times 10^5$
011				7.780		11.33	4	7.80	7.799	-2
110	11.40	4	7.76	7.749	-3	11.43	6	7.74	7.739	+2
020	12.24	4	7.23	7.218	-4	12.29	5	7.20	7.172	-13
$21\bar{1}$ }	19.30	4	4.60	4.604	+8	19.28	6	4.60	4.598	-4
200 }				4.592	-9	19.37	5	4.58	4.596	+36
031				4.267		20.87	1	4.25	4.252	-3
$20\bar{2}$	21.87	10	4.06	4.056	-12	21.85	5	4.06	4.059	-16
$12\bar{2}$				4.042		21.97	9	4.04	4.047	+12
022				3.890		22.84	4	3.890	3.900	+32
220	22.92	5	3.877	3.874	-8	22.98	4	3.867	3.869	+9
102				3.640		24.30	2	3.660	3.660	+3
040	24.63	11	3.612	3.609	-10	24.78	9	3.590	3.586	-17
041				3.361		26.60	5	3.348	3.346	-14
$30\bar{1}$	27.19	9	3.277	3.274	-19	27.22	11	3.273	3.272	-5
003				3.079					3.098	+3
$23\bar{2}$	28.76	7	3.101	3.101	+4	28.80	6	3.097	3.094	-20
300				3.061		29.13	2	3.063	3.064	+7
310	29.80	55	2.996	2.995	-10	29.79	48	2.997	2.996	-2
$22\bar{3}$				2.864		31.12	3	2.871	2.868	-27

TABLE 7 (continued)

hkl	$Mg_2Al_4SiO_{10}$ (this study)					Aluminous sapphirine (Foster)				
	$2\theta_{observed}$	I/I_o	$d_{observed}$	d_{calc}	$\Delta Q \times 10^5$	$2\theta_{observed}$	I/I_o	$d_{observed}$	d_{calc}	$\Delta Q \times 10^5$
042 240	31.43	33	2.844	2.844 2.838	+5 -48	31.47	34	2.840	2.839	-13
212	32.31	14	2.768	2.763	-44	31.56	39	2.832	2.827	-46
$24\bar{2}$	33.25	4	2.692	2.696	+44	32.38	9	2.762	2.758	-38
103				2.650		33.32	5	2.687	2.687	+7
$31\bar{3}$	33.56	3	2.668	2.663	-52	33.61	4	2.664	2.665	+12
301	33.93	4	2.640	2.639	-4	33.68	3	2.659	2.659	+3
033				2.593		33.91	4	2.641	2.646	+51
330	34.77	23	2.578	2.583	+59	34.45	4	2.601	2.600	-15
241				2.559		34.84	18	2.573	2.580	+79
151				2.565		35.08	7	2.556	2.555	-9
$10\bar{4}$	36.55	100	2.456	2.456	-6				2.555	-8
060	37.31	3	2.408	2.406	-29	36.69	100	2.447	2.449	+28
043				2.342		37.64	9	2.388	2.391	+43
$34\bar{2}$	38.20	30	2.354	2.356	+36	38.34	22	2.346	2.344	-23
$12\bar{4}$				2.324					2.349	+58
340	38.52	6	2.335	2.335	-5	38.58	9	2.332	2.334	+36
$42\bar{2}$				2.301					2.329	-35
						39.12	3	2.301	2.229	-29

A low-temperature stability limit of sapphirine in the presence of water (see table 6) is given by its breakdown to the hydrous assemblage chlorite + corundum, which takes place at pressures between 15 and 24 kb below an estimated temperature of 850°C.

It is reasonable that a silica-poor phase such as sapphirine would not coexist with free quartz. This incompatibility holds true throughout the entire pressure stability range investigated at temperatures up to about 1100°C. However, at higher temperatures sapphirines may coexist with free silica by virtue of reactions such as

$$\text{enstatite} + \text{sillimanite} = \text{sapphirine} + \text{quartz}$$

As already mentioned sapphirine + quartz had been obtained by Schreyer and Yoder (1960) as the breakdown assemblage of cordierite at 10 kb, 1200°C. In the present study the stability of this assemblage was confirmed; the univariant equilibrium curve for the above reaction was located in the absence of water at 13 kb and 1110° ± 30°C.

TABLE 8

Comparison of lattice constants of two synthetic sapphirines (see table 4)

	$Mg_2Al_4Si_{10}$ (this study)	Aluminous (Foster no. 8119)
a_o	9.825 ± 0.010 Å	9.820 ± 0.005 Å
b_o	14.437 ± 0.010 Å	14.344 ± 0.006 Å
c_o	9.884 ± 0.015 Å	9.928 ± 0.006 Å
β	110.82 ± 0.08°	110.61 ± 0.04°

Mg-GEDRITE

The synthesis of an orthoamphibole of quaternary composition within the system MgO–Al_2O_3–SiO_2–H_2O was reported by Schreyer (1968). It formed from a variety of bulk compositions and starting materials over the relatively narrow pressure-temperature ranges of 850° to 900°C, 11 to 20 kb. Yields formerly estimated as 85 to 90 percent were prepared from a mixture of talc + kyanite + periclase of the composition $5MgO \cdot 2Al_2O_3 \cdot 6SiO_2$ plus water at 11 kb, 850°C, after 27 hrs (see table 9). The ideal formula of a gedrite of this composition would be $Mg_5Al_2[Al_2Si_6O_{22}](OH)_2$. More recently, however, even higher yields were obtained under similar conditions from a mixture of a less aluminous composition, $6MgO \cdot Al_2O_3 \cdot 7SiO_2$ plus water (see table 9). Since the optical and X-ray properties of these two products were found to be identical, within the limits of error, it is concluded that the composition of the gedrite synthesized approaches more closely that of an ideal formula $Mg_6Al[AlSi_7O_{22}(OH)_2$.

TABLE 9

Selected experimental results bearing on the synthesis and stability of Mg-gedrites

Fluid pressure, kb	Temp., °C	Time, hr	Condensed phases obtained
A. Starting material: Composition $6MgO \cdot Al_2O_3 \cdot 7SiO_2 + xH_2O$ consisting of enstatite and sillimanite with 10% gedrite seeds			
13	900	29	More gedrite, less enstatite and sillimanite
13	920	9	More enstatite and sillimanite, less gedrite
B. Starting material: Composition $6MgO \cdot Al_2O_3 \cdot 7SiO_2 + xH_2O$ consisting of enstatite and kyanite with 10% gedrite seeds			
15.5	880	19	More gedrite, less enstatite and kyanite
15.5	890	30	More enstatite and kyanite, less gedrite
17	870	40	More enstatite and kyanite, less gedrite
18.5	850	47	Less gedrite, more enstatite and kyanite, some talc
19.5	860	15	Enstatite, kyanite, little talc
19.5	900	8	Enstatite, kyanite, trace gedrite
26	880	7	Enstatite, kyanite
C. Starting material: Composition $5MgO \cdot 2Al_2O_3 \cdot 6SiO_2 + xH_2O$ previously crystallized to talc, corundum, and little gedrite			
13	900	9	Enstatite, corundum, more gedrite
19.5	750	63	Talc, chlorite, staurolite, corundum
19.5	850	19	Enstatite, talc, corundum, more gedrite (metastable?)
19.5	900	23	Enstatite, corundum, little kyanite, more gedrite (metastable?)
19.5	925	13	Much gedrite, enstatite, kyanite, corundum
19.5	950	15	Enstatite, corundum, glass
26	850	15	Enstatite, staurolite, talc, trace corundum, same amount gedrite
31.5	850	23	Enstatite, corundum, more gedrite (metastable)
D. Starting material: Composition $6MgO \cdot Al_2O_3 \cdot 7SiO_2 + xH_2O$ consisting of talc, kyanite, and periclase			
14	850	20	Gedrite, traces talc, enstatite, and kyanite
E. Starting material: Composition $5MgO \cdot 2Al_2O_3 \cdot 6SiO_2 + xH_2O$ consisting of talc, kyanite, and periclase			
11	850	27	Gedrite, little kyanite and sapphirine
14	900	3	Gedrite, enstatite, kyanite, sapphirine
17	850	40	Gedrite, talc, kyanite, sapphirine, trace yoderite
19.5	870	15	Enstatite, kyanite, yoderite, staurolite, traces gedrite and talc
25	850	44	Enstatite, staurolite, traces talc and kyanite
F. Starting material: Composition $5MgO \cdot 2Al_2O_3 \cdot 6SiO_2 + xH_2O$ consisting of talc, andalusite, and periclase			
14	860	18	Talc, corundum, little kyanite and gedrite
G. Starting material: Composition $5MgO \cdot 2Al_2O_3 \cdot 6SiO_2 + xH_2O$ consisting of cordierite, periclase, and cristobalite			
11	900	2	Enstatite, cordierite, glass, little gedrite
15	850	25	Enstatite, yoderite, corundum, gedrite

The gedrites synthesized form a felt of minute feathery prisms with somewhat undulatory extinction and positive elongation. Their axial angle could not be measured because of small grain size. The mean refractive index of the felt is 1.618 ± 0.003, and birefringence is estimated as 0.010.

The powder X-ray diffraction pattern of synthetic Mg-gedrites can be distinguished at first glance from that of Mg-anthophyllite, $Mg_7Si_8O_{22}(OH)_2$, by appreciable shifts of peaks toward higher 2θ angles. The detailed measurements are given in table 10, and they were used in the least-squares refinement that yielded the following parameters of the orthorhombic cell:

$$a_o = 18.433 \pm 0.009 \text{ Å} \qquad b_o = 17.807 \pm 0.012 \text{ Å}$$
$$c_o = 5.270 \pm 0.006 \text{ Å}$$

In comparison with Greenwood's (1963) values for pure Mg-anthophyllite ($a_o = 18.61 \pm 0.02$; $b_o = 18.01 \pm 0.06$; $c_o = 5.24 \pm 0.01$ Å), there is thus a marked contraction of the cell in both the a and b directions concomitantly with the substitution AlAl for MgSi, whereas c_o is practically unaffected. It is interesting that a very similar behavior was found for the Al substitution in orthorhombic enstatite (Skinner and Boyd, 1964). Additional experimental work is in progress to demonstrate whether or not other members of the orthoamphibole series exhibiting different compositions and physical properties can be prepared within the system $MgO–Al_2O_3–SiO_2–H_2O$.

Investigations aimed at determining the stability range of the gedrites are severely hampered by the sluggishness of the reactions and the metastable growth of gedrites at the expense of preexisting talc. Thus through the use of talc-bearing starting materials gedrites were obtained over the whole pressure-temperature range 10 to 30 kb, 800° to 925°C. However, runs using talc-free starting materials seeded with synthetic gedrite indicate that a true stability field of this phase is confined to pressures below some 20 kb (see table 9). Nevertheless in most runs in which gedrite is believed to be the stable phase it was accompanied by variable amounts of enstatite and other phases. At temperautres below approximately 800°C, breakdown of the gedrite seeds into talc-bearing assemblages was observed. The high-temperature breakdown of gedrite was found to take place between 850° and 910°C, depending on pressure, and leads to enstatite-bearing assemblages. At pressures in excess of some 15 to 20 kb the stable breakdown assemblages of gedrites are not as yet known: Depending on pressure and temperature parageneses such as talc + enstatite + corundum or talc + pyrope with or without Mg-staurolite may be expected.

The experimental results thus far obtained indicate that gedrites exhibit very similar growth mechanisms and stability relations as their Al-free equivalent anthophyllite, $Mg_7Si_8O_{22}(OH)_2$. Although the first synthesis of Mg-anthophyllite by Bowen and Tuttle (1949) was achieved metastably through breakdown of talc, Greenwood (1963) has demon-

TABLE 10

Powder X-ray diffraction data for synthetic Mg-gedrite made at 11 kb, 850°C, 27 hours, from a composition $5MgO \cdot 2Al_2O_3 \cdot 6SiO_2$ plus water (see table 9.E) (internal Si standard, CuKα radiation)

hkl	$2\theta_{observed}$	I/I_o	$d_{observed}$	d_{calc}	$\Delta Q \times 10^5$
0 2 0	9.91	10	8.925	8.903	-6
2 1 0	10.76	61	8.222	8.185	-13
2 3 0	17.75	4	4.997	4.990	-11
1 1 1	18.20	3	4.874	4.874	-1
4 0 0	19.25	9	4.611	4.608	-5
0 4 0	19.93	34	4.455	4.452	-7
4 2 0	21.72	6	4.092	4.093	+3
1 3 1	23.08	6	3.853	3.854	+1
2 3 1	24.58	21	3.622	3.624	+8
3 3 1	26.86	6	3.319	3.317	-11
4 2 1	27.61	11	3.231	3.232	+10
4 4 0	27.88	32	3.200	3.202	+10
6 1 0	29.51	100	3.027	3.027	+4
5 2 1	31.29	13	2.859	2.861	+17
2 5 1	31.85	18	2.810	2.810	+6
6 3 0	32.85	18	2.726	2.728	+20
3 5 1	33.71	10	2.659	2.660	+13
1 6 1	35.08	12	2.558	2.561	+34
6 4 0	35.47	11	2.531	2.529	-28
4 5 1	36.15	5	2.485	2.485	+4
8 0 0	39.12	8	2.303	2.304	+25
1 7 1	39.63	4	2.274	2.273	-13
4 6 1	40.01	2	2.253	2.255	+30
0 8 0 2 7 1	40.54	3	2.223	2.226 2.223	+50 +3
5 0 2	42.18	5	2.142	2.144	+35
6 6 0 4 3 2	42.30	5	2.137	2.135 2.135	-52 -53
8 0 1	42.83	6	2.111	2.111	+4
5 2 2 7 4 1	43.37	5	2.086	2.084 2.082	-41 -87
8 2 1 4 7 1 0 8 1	44.12	4 b	2.053	2.054 2.052 2.051	+28 -39 -61
6 6 1	45.91	5	1.977	1.978	+35
10 1 0 0 7 2	49.80	7	1.831	1.834 1.830	+83 -29
6 5 2 5 9 0 10 0 1 1 1 3	52.54	3	1.742	1.744 1.743 1.740 1.740	+72 +49 -77 -60
8 6 1 4 9 1 7 4 2 2 1 3	53.27	5	1.720	1.720 1.719 1.718 1.718	+12 -45 -67 -95
9 6 1 5 10 0 8 8 0	57.45*	5	1.603	1.605 1.603 1.601	+123 +18 -105
4 8 2 2 11 0	57.80*	2	1.594	1.596 1.594	+60 +17
4 10 1 7 9 0 4 3 3 0 9 2	58.25*	1	1.583	1.584 1.582 1.582 1.582	+56 -62 -47 -43
2 5 3	59.52*	1	1.552	1.553	+49
5 8 2 11 3 1	59.86*	2	1.544	1.544 1.542	+1 -103

*For these peaks the $CuK\alpha_1$ reflections were measured and used in the calculations.
b = broad.

strated that this phase has a true range of stability in the presence of excess water. This author has also suggested, on the basis of thermochemical calculations, that anthophyllite has an upper pressure stability limit in the vicinity of 20 kb, above which it breaks down to enstatite + talc, an assemblage that contains an equal amount of H_2O. It was found experimentally by the present writers that this breakdown takes place in the pressure range 13 to 19.5 kb.

The stable compatibility relations of gedrites are largely unknown. They will, of course, depend on the extent of solid solution. It is important to note that the presumed line of substitution $AlAl \rightleftharpoons MgSi$ crosses the join $MgSiO_3$–Al_2SiO_5. Since the assemblage quartz + aluminous enstatite with or without Al_2SiO_5 is probably the stable breakdown paragenesis of gedrites at high temperatures, it may be expected that at least the less aluminous gedrites may also coexist with free quartz. On the other hand, more aluminous gedrites might occur in stable assemblage with phases such as Al_2SiO_5, aluminous enstatite, corundum, sapphirine, but not with quartz.

BORON-FREE KORNERUPINE

Kornerupine is a rare natural mineral first discovered near Fiskernaeset, Greenland (Lorenzen, 1884), where it occurs in a gneiss together with sapphirine, gedrite, cordierite, and other phases outside the system discussed here. According to the first chemical analysis Lorenzen attributed the simple formula $MgAl_2SiO_6$ ($=MgO \cdot Al_2O_3 \cdot SiO_2$) to the new mineral species. Later analysis of kornerupine from this and other localities (for example, Lacroix and Gramont, 1919; Hey, Anderson, and Payne, 1941; McKie, 1965), however, always reported appreciable quantities of B_2O_3. Whereas Vogt (1947) has emphasized the probability that boron enters the mineral in definite proportions, the most recent analysis given by McKie (1965) of a kornerupine from Mautia Hill, Tanzania, yielded far less B_2O_3 than necessary to satisfy the formula proposed by Vogt. Kornerupine was first synthesized by Robbins and Yoder (1962) at 5 kb as a high-temperature breakdown product of the tourmaline end-member dravite.

In view of these relationships it is of particular interest that a phase exhibiting all the optical and X-ray characteristics of natural kornerupine was synthesized by the present authors in the systems MgO–Al_2O_3–SiO_2–H_2O. This phase is, therefore, called boron-free kornerupine.[1]

The largest yields (about 80 percent) were obtained in runs at 10 to 13 kb and 825° to 850°C held for 1 to 3 days, starting with the bulk compositions $4MgO \cdot 3Al_2O_3 \cdot 4SiO_2$ and $MgO \cdot Al_2O_3 \cdot SiO_2$ plus water made up from synthetic cordierite and synthetic spinel ($MgAl_2O_4$), with or without periclase (table 11). Boron-free kornerupine also formed from a

[1] Contamination of the sample with boron derived from the boron-nitride of the furnace assembly can be excluded, because the capsules were sealed, and the kornerupine phase has also been synthesized in the boron-free environment of a gas-media apparatus (Schreyer and Yoder, unpub. data, 1968).

variety of other mixtures at fluid pressures as low as 8 kb and as high as 20 kb.

Because of incomplete reactions the exact formula of the synthetic boron-free kornerupine is not as yet known. In particular it cannot be determined which of the available elements substitutes for boron. McKie (1965) suggested the general formula of natural kornerupine to be

$$R_{<2}^{[8,6]}R_4^{[6]}Al_5^{[6,4]}(Al,Si)_4^{[4]}(Si,B)_1^{[4]}(O,OH)_{22}.$$

For the present boron-free kornerupine the site $R^{[8,6]}$ can be either vacant or occupied by Mg leading to the following theoretical compositions:

$$\square_2\ Mg_4\ Al_5\ (Al\ Si_3)\ Si\ O_{20}(OH)_2\ (=4:3:4) \qquad \text{or}$$
$$(\square Mg)\ Mg_4\ Al_5\ (Al\ Si_3)\ Si\ O_{22}\ (=5:3:4)$$

Of these two possibilities, both involving Si for B substitutions, the first one seems preferable because it is the bulk composition that gave better yields. Due to the fact that the natural kornerupine poorest in boron is also the one richest in Al (McKie, 1965) one might, on the other hand, base a theoretical formula on the $Al \rightleftharpoons B$ substitution which could give, for example,

$$\square_2\ (Mg_{3.5}Al_{0.5})\ Al_5\ (AlSi_3)\ Si_{0.5}Al_{0.5})\ O_{20}(OH)_2\ (=1:1:1)$$

As pointed out above this bulk composition also gave high yields of the boron-free kornerupine.

In the first successful structure determination recently published Moore and Bennett (1968), neglecting the boron present in their sample, give the crystallochemical formula of kornerupine as

$$Mg_2^{VI}\ Mg^{VI}\ Al_6^{VI}\ [Si_2O_7]\ [(Al,Si)_2\ AlO_{10}]\ O_4\ (OH)$$

which lies entirely within the system studied here. However, the possible oxide proportions derived from this formula, that is, 6:7:8 through 6:8:6, did not yield kornerupine in synthesis attempts made thus far. It is suggested, therefore, that the replacement of some of the octahedral aluminum by Mg^{VI} is essential to the kornerupine structure, thus leading to the possible formulas

$$Mg_2^{VI}\ Mg^{VI}\ (Mg^{VI}Al_5^{VI})\ Si_2O_7\ (AlSi)\ SiO_{10}\ O_3(OH)_2\ (=4:3:4) \qquad \text{and}$$
$$Mg_2^{VI}\ Mg^{VI}\ (Mg_{0.5}Al_{5.5})^{VI}\ Si_2O_7\ (Al_{0.5}Si_{1.5})\ AlO_{10}\ O_3(OH)_2\ (=1:1:1)$$

The boron-free kornerupines synthesized at a pressure of 13 kb, or lower, form well-developed prisms and needles showing straight extinction and negative elongation. The latter property is most characteristic, as all other orthorhombic prismatic crystals that may appear in the system under similar pressure temperature conditions (that is, enstatite, gedrite, Mg-staurolite, and sillimanite) have positive elongation. The optical orientation is identical with that of natural boron-bearing kornerupines, and the prism axis is *c*. The axial angle 2 V_x could not be measured, although the universal stage work indicated that it is smaller than about 30°. The refractive indices are $\alpha = 1.665$, $\gamma = 1.678$, both $\pm$ 0.003.

TABLE 11

Selected experimental results bearing on the synthesis, composition, and stability of boron-free kornerupine

Fluid pressure, kb	Temp., °C	Time, hr	Condensed phases obtained
A. Starting material: Composition $4MgO \cdot 3Al_2O_3 \cdot 4SiO_2 + xH_2O$ consisting of cordierite, spinel, and periclase			
13	850	22	Kornerupine, little talc, corundum, cordierite, and spinel
13	900	1	Kornerupine, little enstatite, spinel and corundum, trace cordierite
19.5	975	1	Enstatite, corundum, spinel, little kornerupine (quenched liquid)
B. Starting material: Composition $4MgO \cdot 3Al_2O_3 \cdot 4SiO_2 + xH_2O$ consisting of cordierite, kyanite, and periclase			
13	850	15	Talc, gedrite, sapphirine, kyanite, traces cordierite and corundum
C. Starting material: Composition $4MgO \cdot 3Al_2O_3 \cdot 4SiO_2 + xH_2O$ consisting of cordierite, andalusite, and periclase			
13	850	7	Talc, corundum, spinel, trace chlorite
D. Starting material: Composition $MgO \cdot Al_2O_3 \cdot SiO_2 + xH_2O$ consisting of cordierite and spinel			
10*	825	72	Kornerupine, little talc, enstatite, corundum, and spinel
E. Starting material: Composition $MgO \cdot Al_2O_3 \cdot SiO_2 + xH_2O$ consisting of cordierite, periclase, and γ-Al_2O_3			
13	850	16	Enstatite, corundum, trace gedrite
F. Starting material: Composition $5MgO \cdot 3Al_2O_3 \cdot 4SiO_2 + xH_2O$ consisting of cordierite, spinel, and periclase			
13	800	54	Cordierite, spinel, chlorite, corundum
13	850	19	Kornerupine, enstatite, spinel
19.5	800	13	Talc, spinel, staurolite, chlorite, corundum
19.5	850	40	Enstatite, spinel, kornerupine (quenched liquid?)
19.5	975	1	Enstatite, spinel, kornerupine (quenched liquid)
19.5	975	21	Enstatite, sapphirine, spinel, corundum, kornerupine (quenched liquid)
19.5	975	1.5	Enstatite, spinel, corundum, sapphirine (slow quench)
G. Starting material: Composition $6MgO \cdot 7Al_2O_3 \cdot 8SiO_2 + xH_2O$ consisting of cordierite, spinel, and andalusite			
13	850	52	Talc, corundum, trace cordierite
H. Starting material: Composition $4MgO \cdot 4Al_2O_3 \cdot 3SiO_2 + xH_2O$ consisting of cordierite and spinel			
19.5	975	1	Enstatite, sapphirine, spinel, corundum
I. Starting material: Composition $4MgO \cdot 5Al_2O_3 \cdot 7SiO_2 + xH_2O$ consisting of cordierite, talc, corundum, and 10 wt % yoderite seeds			
8*	800	168	Cordierite, kornerupine, corundum, talc, sapphirine, trace spinel
9*	800	168	Cordierite, kornerupine, corundum, trace sapphirine

*Runs performed in gas-media apparatus.

TABLE 12

Powder X-ray diffraction data for synthetic boron-free kornerupine prepared at 13 kb, 850°C, 22 hr, from a composition $4MgO \cdot 3Al_2O_3 \cdot 4SiO_2$ plus water (see table 11.A) (internal Si standard, CuKα radiation)

hkl	$2\theta_{observed}$	I/I_o	$d_{observed}$	d_{calc}	$\Delta Q \times 10^5$
110	8.42	25	10.501	10.463	-7
200	10.93	5	8.094	8.074	-8
020	12.88	14	6.873	6.868	-3
220	16.92	2	5.240	5.231	-12
310	17.69	1	5.014	5.011	-4
130	20.11	2	4.415	4.405	-24
221	21.50	3	4.133	4.136	+8
400	22.02	3	4.037	4.037	+1
040	25.94	31	3.435	3.434	-4
002	26.42	29	3.373	3.377	+18
112	27.79	3	3.210	3.214	+21
022	29.49	46	3.029	3.030	+11
312	31.97	3	2.799	2.800	+10
150	33.07	10	2.709	2.708	-4
530	33.98	100	2.638	2.639	+9
441	36.87	33	2.438	2.439	+18
042	37.38	3	2.406	2.408	+30
023	42.20	3	2.141	2.139	-43
640	42.72	21	2.117	2.118	+35
602	42.92	10	2.107	2.105	-54
550	43.25	18	2.090	2.093	+15
551	45.39	2	1.998	1.999	+18
170	46.67	1	1.946	1.948	+48

The powder X-ray diffraction data for synthetic boron-free kornerupine, distinct from those of all other phases in the system, are given in table 12. The reflections were indexed on the basis of the orthorhombic unit cell recently defined by McKie (1965). Least-squares refinement resulted in the following lattice constants:

$$a_o = 16.147 \pm 0.010 \text{ Å} \qquad b_o = 13.736 \pm 0.006 \text{ Å}$$
$$c_o = 6.754 \pm 0.004 \text{ Å}$$

In comparison with McKie's (1965) values for the Mautia Hill kornerupine ($a_o = 16.100$; $b_o = 13.767$; $c_o = 6.735$ Å; all $\pm$ 0.002) an expansion of the cell in both the a and c directions and a contraction in the b direction is noted. These differences probably do not result solely from the boron replacement but may be due partly to ferric iron and, possibly, different OH contents in the natural mineral. The cell parameters of other natural kornerupines (Hey, Anderson, and Payne, 1941; Bartl, 1965) are consistently somewhat smaller than those determined for the synthetic boron-free phase.

The experimental data compiled in table 11 do not yield conclusive evidence concerning the stability relations of the boron-free kornerupine.

It is possible, however, that a small stability field exists at relatively low pressures of perhaps 8 to 13 kb and temperatures near 850°C. At higher pressures (near 20 kb) the kornerupine phase was obtained only as a quench product from liquids lying close to the 4:3:4 composition. The failure of the phase to form under subsolidus conditions is considered evidence for its metastability at these pressures; the stable assemblages are either enstatite + corundum or pyrope + corundum. It should also be emphasized that the reactions involving boron-free kornerupine within its possible stability field at low pressures have not been reversed. Therefore, the possibility that boron-free kornerupine is a metastable phase, under these and perhaps under any conditions, cannot be ruled out.

Boron-free kornerupine may coexist, stably or metastably, with sapphirine, enstatite, gedrite, talc, cordierite, corundum, and, possibly, yoderite, but not with quartz. These parageneses are very similar to those encountered in natural environments such as Fiskernaeset, Greenland, and Sakeny, Madagascar, for which the rock name "sakenite" (Lacroix, 1939) and even a separate mineral facies, the "sakenite facies" (Vogt, 1947), had been proposed. The incompatibility of the boron-free kornerupine with quartz is apparently also valid for most boron-containing natural kornerupines (Vogt, 1947) and possibly even for the variety prismatine that contains Na (Scheumann, 1960). It is suggestive that such incompatibility might also be one reason for the rarity of natural kornerupines, which may be replaced, in the presence of Na and excess silica, by the common boron-bearing mineral tourmaline known to coexist with free quartz. The association of kornerupine with interstitial quartz, tourmaline, and biotite described from Port Shepstone, Natal (de Villiers, 1940), might be the result of an incomplete replacement of the above kind during a later introduction of silica.

PYROPE

The synthesis of the pure MgAl-garnet, pyrope, was achieved as early as 1955 by Coes; its stability range in the anhydrous system MgO–Al_2O_3–SiO_2 at high temperatures up to its melting point was worked out by Boyd and England (1959). An extension of the pyrope stability to lower temperatures and pressures in the presence of water was reported by Schreyer (1968) and is shown here as figure 6. Experimental results are compiled in table 13. The low-temperature stability limit in the presence of excess water is probably defined by two breakdown reactions, (1) to yoderite + talc + chlorite and (2) to kyanite + talc + chlorite both originating from an invariant point that is also the origin of the low-temperature breakdown curves of yoderite as shown in figure 5. In the water-deficient region pyrope must be stable to even lower temperatures.

The low-pressure stability limit of pyrope at relatively low temperatures apparently has a very similar slope as that reported by Boyd and England (1959) for higher temperatures, although there must be

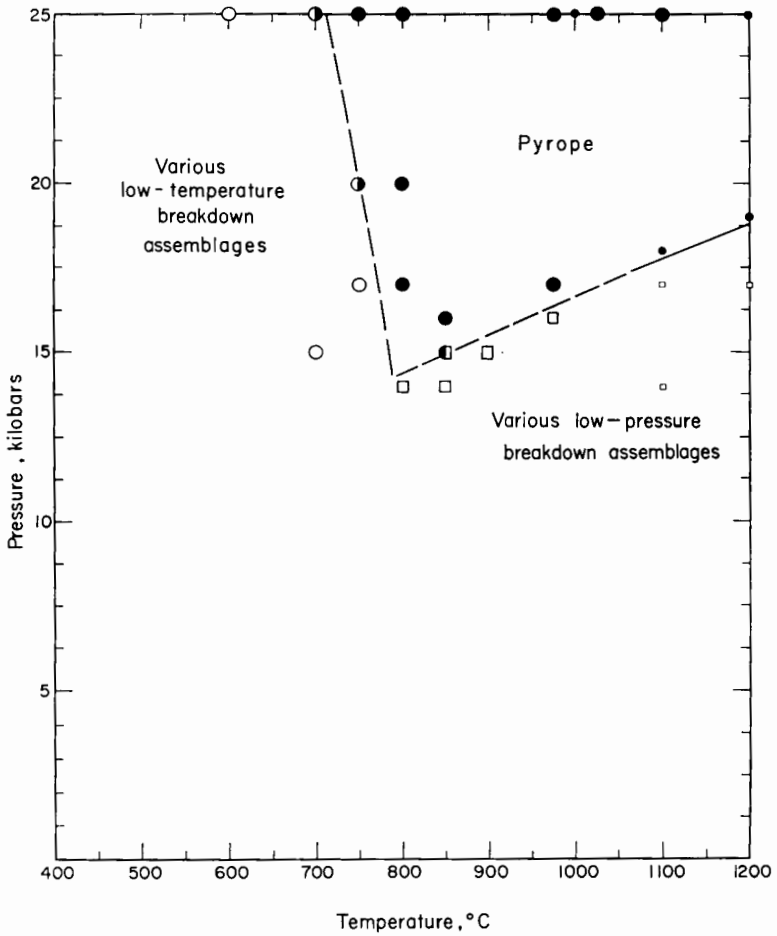

Fig. 6. Preliminary pressure-temperature diagram for the stability of pyrope in the presence of water based on runs seeded with synthetic pyrope. Solid dots indicate growth of pyrope; open circles, breakdown to low-temperature assemblages; open boxes, breakdown to low-pressure assemblages; composite symbols indicate negligible reaction of pyrope seeds. The smaller symbols represent experimental results reported by Boyd and England (1959); the solid line is their breakdown curve, which is connected with the breakdown curve based on the more recent results (Schreyer, 1968) through a minor discontinuity.

changes in the breakdown assemblages. However, the stable breakdown reactions in the presence of excess water are not as yet fully defined. One of the most confusing aspects of the experimental results is the synthesis of hydrous breakdown products of pyrope, such as talc or gedrite, at temperatures above those of the supposed pyrope stability field.

There are two possible explanations for this behavior: (1) The low-temperature end of the pyrope breakdown curve, in the range 800° to 900°C as illustrated in figure 6, may be the metastable extension of the

stable high-temperature breakdown to anhydrous assemblages. This curve would extend stably to lower temperature only under conditions of water deficiency. (2) The pyrope grown at the lowest temperatures (800°-850°C) in small amounts is not an anhydrous phase but a hydrogarnet. A more detailed study involving longer runs with various seed assemblages, as well as analytical work, is necessary to resolve this problem.

Direct and complete synthesis of euhedral pyrope in the presence of water is rapidly achieved at pressures near 25 kb and temperatures of the order of 1000°C (table 13). The starting material used was the low-pressure assemblage cordierite + spinel + forsterite crystallized from glass of pyrope composition at 1 atm.

TABLE 13

Selected experimental results bearing on the synthesis and stability of pyrope

Fluid pressure, kb	Temp., °C	Time, hr	Condensed phases obtained
A. Starting material: Composition $3MgO \cdot Al_2O_3 \cdot 3SiO_2 + xH_2O$ previously crystallized to cordierite, spinel, and forsterite; with 10 wt % pyrope seeds added			
14	800	72	Enstatite, yoderite, talc, chlorite, corundum, small trace pyrope
14	850	46	Enstatite, gedrite, corundum, sapphirine, less pyrope
15	700	66	Chlorite, talc, yoderite
15	850	23	Enstatite, gedrite, trace yoderite and sapphirine (?), same amount pyrope
15	900	17	Enstatite, corundum, trace sapphirine
16	850	20	Enstatite, gedrite, corundum, more pyrope
16	975	16	Enstatite, trace sapphirine, boron-free kornerupine (quenched liquid)
17	750	65	Chlorite, talc, yoderite
17	800	44	Enstatite, yoderite, little chlorite, more pyrope
17	975	20	Pyrope, enstatite, sapphirine, glass, little corundum
20	750	28	Chlorite, talc, yoderite, same amount pyrope
20	800	17	Chlorite, enstatite, staurolite, yoderite, more pyrope
25	600	65	Chlorite, talc, yoderite, staurolite
25	700	26	Chlorite, talc, staurolite, trace yoderite, same amount pyrope
25	750	22	Chlorite, talc, staurolite, more pyrope
B. Starting material: Composition $3MgO \cdot Al_2O_3 \cdot 3SiO_2 + xH_2O$ consisting of cordierite, spinel, and forsterite, no pyrope seeds			
25	800	22	Enstatite, staurolite, chlorite
25	1025	2	All pyrope

TABLE 14

Physical constants of pyrope according to various authors

	a_o, Å	n
Skinner (1956)	11.459 ± 0.001	1.714 ± 0.002
Boyd and England (1959)	11.456 ± 0.002	1.710 ± 0.003
This study	11.464 ± 0.001	1.705 ± 0.002

The physical constants of pyrope synthesized at 25 kb, 1000°C, 2 hrs, in a hydrous environment are listed in table 14, together with those given by other authors. Although the lattice constants are in reasonable agreement, the pyrope synthesized here has a significantly lower refractive index, which might indeed indicate the incorporation of some OH as hydrogarnet component under the conditions studied.

The preliminary results on the stability field of pyrope discussed earlier supports the general view that for any reasonable geothermal gradient pure pyrope can be formed only within the Earth's mantle, regardless of the presence or absence of water. However, in the presence of water, a minimum temperature of some 750°C and a minimum depth of about 60 km must be attained. At the appropriate pressures and temperatures, pyrope may coexist with every other magnesian and aluminous phase of the system, except cordierite and, probably, boron-free kornerupine. A notable feature is, however, its incompatibility with free silica (Boyd and England, 1963; Schreyer, 1968) at least over the pressure-temperature range in which quartz is the stable polymorph. At a pressure of 40 kb pyrope was found to coexist with coesite (Boyd and England, 1963).

CONCLUDING REMARKS

Under the conditions of elevated pressures, that is, about 8 to 25 kb, and intermediate temperatures, that is, about 700°-1200°C, the following compounds must be considered in any discussion of phase relations in the system MgO–Al_2O_3–SiO_2–H_2O: quartz, (aluminous) talc, anthophyllite-gedrite, (aluminous) enstatite, forsterite, periclase, brucite, spinel, corundum, kyanite, sillimanite, cordierite, pyrope, yoderite, Mg-staurolite, boron-free kornerupine, chlorite, and sapphirine. The phases sepiolite, stevensite, serpentine, boehmite, diaspore, kaolinite, pyrophyllite, and montmorillonite can be neglected because their stability ranges lie at generally lower temperatures. Andalusite and mullite are confined to lower pressures. The stability relations of the phase β-alumina within the system studied are not known.

There are thus 18 crystalline phases that may form stable subsolidus assemblages over limited pressure-temperature ranges. Theoretically the maximum number of assemblages, including those metastable, is 816. They would be related to each other through 3060 univariant curves and 8568 invariant points, if one neglects the many cases of degeneration and assumes a vapor phase as omnipresent. The number of stable assemblages, univariant curves, and invariant points will, therefore, be much smaller. In addition, some assemblages can be ruled out, because the stability fields of the phases involved do not overlap. Such forbidden assemblages are: Cordierite-pyrope, cordierite-Mg-staurolite, and, probably, boron-free kornerupine-pyrope. Nonetheless, it is clear that the phase relations within this system of only four components will be extremely complicated. Much detailed work has yet to be done to provide a fully satisfactory picture, even of the breakdown assemblages of the phases described in the present paper.

In recent speculations on the chemical compositions constituting the Earth's mantle the authors (for example, Ringwood, 1959; Birch, 1965; MacGregor, 1967) agree that some 80 to 90 percent of the possible mantle material fall within the system MgO–Al_2O_3–SiO_2. Of these three components Al_2O_3, amounting only to some 4 percent, is the least important. Therefore, the hypothetical mantle rocks will project predominantly into the Mg-rich portion of the ternary diagram, probably into the triangle formed by the three phases forsterite, enstatite, and pyrope (Schreyer, 1966). In contrast to these highly magnesian compositions, the high-pressure phases described in the present paper are more aluminous, and most of them contain essential structural water. Although the occurrence of micas in rocks believed to have been ejected from the mantle certainly suggests the availability of water, at least locally, at those depths, the high alumina contents of the new phases described seem to preclude their appearance within the Earth's mantle to any large extent. However, even local alumina enrichments of the mantle are suggested through the finding of corundum-bearing eclogite xenoliths in kimberlites (N. V. Sobolev, 1964) as well as of garnet-corundum-kyanite assemblages occurring in grospydite xenoliths from these same rocks (Sobolev, Kuznetsova, and Zyuzin, 1968).

Discussion of the potential occurrence of the aluminous high-pressure phases in mantle rocks will, at any rate, depend on a more detailed knowledge of the compatibility relations between the solid phases within the system MgO–Al_2O_3–SiO_2–H_2O as a function of pressure and temperature than is presently available. Preliminary experimental results indicate that, in the presence of water, chlorite, and in its absence, pyrope, may contain most of the alumina available in mantle rocks. Critical tie lines that would, for compositions poor in alumina, prohibit the occurrence of the highly aluminous hydrous phases described here in mantle rocks are enstatite-spinel and forsterite-pyrope. These two assemblages were found to be stable in the anhydrous system at temperatures above 1000°C at low and high confining pressures, respectively (MacGregor, 1964). They are believed by Ringwood, MacGregor, and Boyd (1964) to represent the main criteria governing the mineralogy of the uppermost mantle. However, if these two assemblages were not stable in the presence of water at temperatures in the approximate range 800° to 1000°C, there might indeed be a possibility that the phases gedrite, boron-free kornerupine, yoderite, Mg-staurolite, and sapphirine appear in stable coexistence with enstatite and, possibly, even with forsterite over limited pressure-temperature ranges. The stable coexistence of enstatite even with corundum was verified in the present study under conditions outside the stability fields of both boron-free kornerupine and pyrope, Thus the possibility of the appearance of aluminous minerals other than spinel and pyrope even in mantle compositions poor in alumina should be taken into account. If these minerals are also hydrous, they may provide an effective depository for the mobile component water in subcrustal material.

Yoderite, Al-poor sapphirine, and the kornerupine of lowest boron content yet discovered were described by McKie (1959, 1963, 1965) from Mautia Hill, Tanzania, where they occur in metamorphic rocks believed to be of crustal origin. These occurrences demonstrate that the pressure-temperature conditions required for the formation of these minerals were attained within a deep zone of an old Precambrian orogenic belt. Therefore, the geological environments most likely to carry the aluminous high-pressure phases described in this paper will be the lowermost portions of deeply buried geosynclines, in which aluminous rocks of metasedimentary origin were subjected to metamorphism.

ACKNOWLEDGMENTS

The present work was inaugurated by one of us (W. Schreyer) at the Geophysical Laboratory, Washington, D. C., during the tenure of a Fellowship from the Carnegie Institution of Washington during the period August 1966 to May 1967. Particular thanks are due to Dr. H. S. Yoder, Jr., of the Geophysical Laboratory, who not only made available his solid-media apparatus and some of the starting materials used but also stimulated and actively promoted this work through his interest in the mineral named in his honor. The study was continued at Kiel, Germany, using a solid-media apparatus of identical design supplied through a grant by Deutsche Forschungsgemeinschaft, Bad Godesberg. Dr. I. D. MacGregor, Dallas, Texas, has kindly loaned a replacement pressure vessel which enabled us to bring the study at least to a productive, yet preliminary, stage before the manuscript for this volume, dedicated to Dr. J. F. Schairer, had to be submitted. Dr. H. R. Shell, U. S. Bureau of Mines, College Park, Md., generously made available some of the high-purity spinel used as a starting material. Professor W. R. Foster, Ohio State University, contributed a sample of synthetic sapphirine for X-ray study. The X-ray data given in this paper were refined at Deutsches Rechenzentrum, Darmstadt, using a least-squares program provided by Professor C. W. Burnham, Harvard University. Some of the data on sapphirine reported here were obtained in cooperation with Dipl. Min. D. Ackermand, Kiel, who has initiated work for a doctor's thesis on this mineral. A 2V determination was kindly performed by Dipl. Geol. M. Raith, Kiel. The authors gratefully acknowledge the review of the manuscript by Drs. G. A. Chinner, Cambridge, England, and S. W. Richardson, Edinburgh, Scotland.

REFERENCES

Bartl, H , 1965, Zur Kornerupinstruktur: Neues Jahrb. Mineralogie Monatsh. p. 151-153.

Birch, F., 1965, Speculations on the Earth's thermal history: Geol. Soc. America Bull., v. 76, p. 133-154.

Bowen, N. L., and Tuttle, O. F., 1949, The system MgO–SiO_2–H_2O: Geol. Soc. America Bull., v. 60, p. 439-460.

Boyd, F. R., and England, J. L., 1959, Pyrope: Carnegie Inst. Washington Year Book v. 58, p. 83-87.

———— 1960a, Aluminous enstatite: Carnegie Inst. Washington Year Book 59, p 49-52.

Boyd, F. R., and England, J. L., 1960b, Apparatus for phase-equilibrium measurements at pressures up to 50 kilobars and temperatures up to 1750°C: Jour. Geophys. Research, v. 65, p. 741-748.

———— 1961, Melting of silicates at high pressures: Carnegie Inst. Washington Year Book 60, p. 113-125.

———— 1963, Some effects of pressure on the phase relations in the system MgO–Al_2O_3–SiO_2: Carnegie Inst. Washington Year Book 62, p. 121-124.

Burnham, C. W., 1962, Lattice constant refinement: Carnegie Inst. Washington Year Book 61, p. 132-135.

Coes, L., 1955, High pressure minerals: Am. Ceramic Soc. Jour., v. 38, p. 298.

de Villiers, J. E., 1940, Iron-rich kornerupine from Port Shepstone, Natal: Mineralog. Mag., v. 25, p. 550-556.

Fawcett, J. J. ,and Yoder, H. S., Jr., 1966, Phase relationships of chlorites in the system MgO–Al_2O_3–SiO_2–H_2O: Am. Mineralogist, v. 51, p. 353-380.

Fleet, S. G., 1967, Non-space-group absences in sapphirine: Mineralog. Mag., v. 36, p. 449-450.

Fleet, S. G. and Megaw, H. D., 1962, The crystal structure of yoderite: Acta Cryst., v. 15, p. 721-728.

Foster, W. F., 1950a, Synthetic sapphirine and its stability field in the system MgO–Al_2O_3–SiO_2: Jour. Geology, v. 58, p. 135-151.

———— 1950b, Synthetic sapphirine and its stability field in the system MgO–Al_2O_3–SiO_2: Am. Ceramic Soc. Jour., v. 33, p. 73-84.

Gossner, B., and Mussgnug, F., 1928, Vergleichende röntgenographische Untersuchungen von Magnesiumsilikaten: Neues Jahrb. Mineralogie Beil-Bd. 58, A, p. 213.

Greenwood, H. J., 1963, The synthesis and stability of anthophyllite: Jour. Petrology, v. 4, p. 317-351.

Hannemann, R. E., and Strong, H. M., 1965, Pressure dependence of the emf of thermocouples to 1300°C and 50 kbar: Jour.Appl. Physics, v. 36, p. 523-528.

Hey, M. H., Anderson, B. W., and Payne, C. J., 1941, Some new data concerning kornerupine and its chemistry: Mineralog. Mag., v. 26, p. 119-130.

Keith, M. L., and Schairer, J. F., 1952, The stability field of sapphirine in the system MgO–Al_2O_3–SiO_2: Jour. Geology, v. 60, p. 181-186.

Kerr, P. F., and Callaghan, E., 1935, Scheelite-leuchtenbergite vein in Paradise Range, Nevada: Geol. Soc. America Bull., v. 46, p. 1957-1974.

Kuzel, H. J., 1961, Über Formel und Elementarzelle des Sapphirin: Neues Jahrb. Mineralogie Monatsh., p. 68-71.

Lorenzen, J., 1884, Undersögelse av Mineralier fra Grönland: Medd. om Grönland, v. 7, p. 1.

Lacroix, A., 1939, Sur un nouveau type de roches metamorphiques (saknite) faisant partie des schistes cristallins du Sud de Madagascar: Acad. Sci. Comptes rendus, v. 209, p. 609.

Lacroix, A., and Gramont, A., 1919, Sur la présence du bore dans quelques silica-aluminates basiques naturels: Acad. Sci. Comptes rendus, v. 168, p. 857.

MacGregor, I. D., 1964, The reaction 4 enstatite + spinel = forsterite + pyrope: Carnegie Inst. Washington Year Book 63, p. 156-157.

———— 1967, Mineralogy of model mantle compositions, *in* Wyllie, P. J., ed., Ultramafic and related rocks: New York, John Wiley & Sons, p. 382-393.

McKie, D., 1959, Yoderite, a new hydrous magnesium iron alumino-silicate from Mautia Hill, Tanganyika: Mineralog. Mag., v. 32, p. 282-307.

———— 1963, Order-disorder in sapphirine: Mineralog. Mag., v. 33, p. 635-645.

———— 1965, The magnesium aluminum borosilicates: kornerupine and grandiderite: Mineralog. Mag., v. 34, p. 346-357.

McKie, D., and Bradshaw, N., 1966, A green variety of yoderite: Nature, v. 210, p. 1148.

Moore, P. B., and Bennett, J. M., 1968, Kornerupine: Its crystal structure: Science, v. 159, p. 524-526.

Náray-Szabó, I., and Sasvári, K., 1958, On the structure of staurolite $HFe_2Al_9Si_4O_{24}$: Acta Cryst., v. 11, p. 862-865.

Rankin, G. A., and Merwin, H. E., 1918, The ternary system MgO–Al_2O_3–SiO_2: Am. Jour. Sci., 4th ser., v. 45, p. 301-325.

Richardson, S. W., 1967, Staurolite: Carnegie Inst. Washington Year Book 65, p. 248-252.

———— 1968, The composition of synthetic Fe-staurolite: Carnegie Inst. Washington Year Book 66, p. 391-398.

Ringwood, A. E., 1959, On the chemical evolution and densities of the planets: Geochim. et Cosmochim. Acta, v. 15, p. 256-284.

Ringwood, A. E., MacGregor, I. D., and Boyd, F. R., 1964, Petrological constitution of the upper mantle: Carnegie Inst. Washington Year Book 63, p. 147-152.

Robbins, C. R., and Yoder, H. S., Jr., 1962, Stability relations of dravite, a tourmaline: Carnegie Inst. Washington Year Book 61, p. 106-107.

Roy, D. M., and Roy, Rustum, 1955, Synthesis and stability of minerals in the system MgO–Al_2O_3–SiO_2–H_2O: Am. Mineralogist, v. 40, p. 147-178.

Scheumann, K. H., 1960, Das Kornerupingestein von Waldheim in seinem genetischen Zusammenhang: Leipzig Akad. Wiss. Abh. sächs., v. 47, no. 2, 23 p.

Schreyer, W., 1966, Zur mineralogischen Konstitution des Erdmantels: Naturw. Rundschau, v. 19, p. 184-189.

———— 1968, A reconnaissance study of the system MgO–Al_2O_3–SiO_2–H_2O at pressures between 10 and 25 kb: Carnegie Inst. Washington Year Book 66, p. 380-392.

Schreyer, W., and Schairer, J. F., 1961a, Metastable solid solutions with quartz-type structures on the join SiO_2–$MgAl_2O_4$: Zeitschr. Kristallographie, v. 116, p. 60-82.

———— 1961b, Compositions and structural states of anhydrous Mg-cordierites. A reinvestigation of the central part of the system MgO–Al_2O_3–SiO_2: Jour. Petrology, v. 2, p. 324-406.

———— 1962, Metastable osumilite- und petalite-type phases in the system MgO–Al_2O_3–SiO_2: Am. Mineralogist, v. 47, p. 90-104.

Schreyer, W., and Seifert, F., 1969, Compatibility relations of the aluminum silicates in the system MgO–Al_2O_3–SiO_2–H_2O and K_2O–MgO–Al_2O_3–SiO_2–H_2O at high pressures: Am. Jour. Sci., v. 267, p. 371-388.

Schreyer, W., and Yoder, H. S., Jr., 1960, Instability of anhydrous Mg-cordierite at high pressures: Carnegie Inst. Washington Year Book 59, p. 90-91.

———— 1964, The system Mg-cordierite–H_2O and related rocks: Neues Jahrb. Mineralogie Abh., v. 101, p. 271-342.

———— 1968, Yoderite: Synthesis, stability and interpretation of its natural occurrence: Carnegie Inst. Washington Year Book 66, p. 376-380.

Segnit, E. F., 1957, Sapphirine-bearing rocks from MacRobertson Land, Antarctica: Mineralog. Mag., v. 31, p. 690-697.

Skinner, B. J., 1956, Physical properties of end members of the garnet group: Am. Mineralogist, v. 41, p. 428-436.

Skinner, B. J. and Boyd, F. R., 1964, Aluminous enstatites: Carnegie Inst. Washington Year Book 63, p. 163-165.

Sobolev, N. V., 1964, Eclogite xenolith with ruby (in Russian): Acad. Sci. USSR Doklady, v. 157, 1382-1384.

Sobolev, N. V., Kuznetsova, I. K., and Zyuzin, N. I., 1968, The petrology of grospydite xenoliths from the Zagadochnaya kimberlite pipe in Yakutia: Jour. Petrology, v. 9, p. 253-280.

Vogt, T., 1947, Mineral assemblages with sapphirine and kornerupine: Comm. géol. Finlande Bull., v. 140, p. 15-24.

Yoder, H. S., Jr., 1952, The MgO–Al_2O_3–SiO_3–SiO_2–H_2O system and the related metamorphic facies: Am. Jour. Sci., Bowen v., p. 569-627.